Validating a 1-D SVAT model in a range of USA and Australian ecosystems: evidence towards its use as a tool to study Earth's system interactions

Petropoulos, George; North, Matthew; Ireland, Gareth; Srivastava, Prashant K.; Rendall, Daisy Veronica

Published in:
Geoscientific Model Development

DOI:
10.5194/gmdd-8-2437-2015

Publication date:
2015

Citation for published version (APA):
Petropoulos, G., North, M., Ireland, G., Srivastava, P. K., & Rendall, D. V. (2015). Validating a 1-D SVAT model in a range of USA and Australian ecosystems: evidence towards its use as a tool to study Earth's system interactions. *Geoscientific Model Development*, *8*, 2437–2495. https://doi.org/10.5194/gmdd-8-2437-2015

Geosci. Model Dev. Discuss., 8, 2437–2495, 2015
www.geosci-model-dev-discuss.net/8/2437/2015/
doi:10.5194/gmdd-8-2437-2015

Geoscientific Model Development Discussions
Open Access

Validating a 1-D SVAT model in a range of USA and Australian ecosystems: evidence towards its use as a tool to study Earth's system interactions

G. P. Petropoulos[1], M. R. North[1], G. Ireland[1], P. K. Srivastava[2,3], and D. V. Rendall[1]

[1]Department of Geography and Earth Sciences, Aberystwyth University, Aberystwyth, SY23 3DB, UK
[2]Hydrological Sciences Branch, NASA Goddard Space Flight Center, Greenbelt, Maryland, USA
[3]Earth System Science Interdisciplinary Center, University of Maryland, Maryland, USA

Received: 9 January 2015 – Accepted: 12 February 2015 – Published: 5 March 2015

Correspondence to: G. P. Petropoulos (george.petropoulos@aber.ac.uk)

Published by Copernicus Publications on behalf of the European Geosciences Union.

Abstract

This paper describes the validation of the SimSphere SVAT model conducted at different ecosystem types in the USA and Australia. Specific focus was given to examining the models' ability in predicting Shortwave Incoming Solar Radiation (R_g), Net Radiation (R_{net}), Latent Heat (LE), Sensible Heat (H), Air Temperature at 1.3 m ($T_{air\,1.3\,m}$) and Air Temperature at 50 m ($T_{air\,50\,m}$). Model predictions were compared against corresponding in situ measurements acquired for a total of 72 selected days of the year 2011 obtained from 8 sites belonging to the AmeriFlux (USA) and OzFlux (Australia) monitoring networks. Selected sites were representative of a variety of environmental, biome and climatic conditions, to allow for the inclusion of contrasting conditions in the model evaluation.

The application of the model confirmed its high capability in representing the multifarious and complex interactions of the Earth system. Comparisons showed a good agreement between modelled and measured fluxes, especially for the days with smoothed daily flux trends. A good to excellent agreement between the model predictions and the in situ measurements was reported, particularly so for the LE, H, $T_{air\,1.3\,m}$ and $T_{air\,50\,m}$ parameters (RMSD = 39.47, 55.06 W m^{-2}, 3.23, 3.77 °C respectively). A systematic underestimation of R_g and R_{net} (RMSD = 67.83, 58.69 W m^{-2}, MBE = 67.83, 58.69 W m^{-2} respectively) was also found. Highest simulation accuracies were obtained for the open woodland savannah and mulga woodland sites for most of the compared parameters. Very high values of the Nash–Sutcliffe efficiency index were also reported for all parameters ranging from 0.720 to 0.998, suggesting a very good model representation of the observations.

To our knowledge, this study presents the first comprehensive validation of SimSphere, particularly so in USA and Australian ecosystem types. Findings are important and timely, given the rapidly expanding use of this model worldwide both as an educational and research tool. This includes ongoing research by different Space Agencies

examining its synergistic use with Earth Observation data towards the development of global operational products.

1 Introduction

The importance of studying land surface interactions to develop a better understanding of Earth's physical processes and feedbacks is evident from several investigations. Today, particularly so in the face of climate change, it has been recognised by the global scientific community as a topic requiring further attention and investigation (Battrick et al., 2006; Petropoulos et al., 2014). The importance of this work is documented within numerous scientific disciplines, and a further understanding of land surface interactions is of crucial importance to help address directives such as the European Parliament "Directive 2000/60/EC", aimed at establishing a framework for community action in the field of water policy, namely the EU Water Framework Directive. Furthermore, Space Agencies have also been trying to identify how they can potentially contribute to research in this field. One example being the European Space Agency (ESA), which via its Living Planet programme has identified a number of scientific challenges covering different aspects of the Earth system on which the Agency hopes to provide significant contributions (ESA, 1999). On this basis, the need to develop a holistic understanding of how land surface parameters characterising the planet's energy and water budget in different ecosystems has never been more important (WMO, 2002; ESA, 2014).

Generally, the requirement for accurate information on such parameters can be addressed by two efforts: (1) in the field by obtaining actual measurements, and (2) by development and validation of models (Zhan et al., 2003; Verbeek et al., 2008). However, obtaining reliable measurements of those parameters can be very cumbersome, if not in some cases impractical, as they are characterised by certain limitations (e.g. see recent review by Petropoulos et al., 2013e). On the other hand, mathematical models have been proven useful in providing estimates of those parameters. Indeed, models are characterised by certain advantages including their ability to estimate the behaviour

GMDD
8, 2437–2495, 2015

of complex terrain ecosystems which cannot be derived by normal logic. Furthermore, they have an ability to extrapolate results and study various hypothetical scenarios. These advantages allow situating knowledge of certain phenomena in a broader context (Verbeek et al., 2008). A representative description of land surface interactions requires mathematical models capable of accurately describing the physical and biological processes in the soil–vegetation–atmosphere continuum (Olchev et al., 2008; Petropoulos, 2013). One of the main goals of modellers in the area of environmental studies is to improve our understanding of complex natural systems and advance the development and application of models that simplify the representation of the real world systems under study (Silberstein, 2006; Sheikh et al., 2009). This recognition of the importance for a better understanding of the biophysical mechanisms of land surface–atmosphere interactions has motivated the rapid progress in environmental mathematical modelling over the past few decades (Stoyanova and Georgiev, 2013; Koirala et al., 2014). Indeed, significant progress has been made towards the development of models able to describe the processes between the vegetation, soil, and the atmosphere of the Earth's system (Bellocchi et al., 2010; Stoyanova and Georgiev, 2013).

Land surface parameterisation schemes (LSPs, also known as land surface models (LSMs)) are one of the preferred scientific tools to quantify, at fine spatial and temporal resolutions, Earth system interactions. Such modelling schemes simulate a number of parameters characterising land surface feedbacks and processes within the lower atmospheric boundary from a predefined set of surface characteristics (i.e. properties of soil, vegetation and water). LSPs have begun to emerge as valuable tools in a number of associated fields within environmental sciences. Often LSP's are utilised, amongst others, to assess water resources, to evaluate the hydrological impacts of changes in climate and land use, to model land atmosphere exchanges and emissions of aerosols (Prentice et al., 2014). Early LSP models generally represented the surface effect on the atmosphere or were based on simple approximate equations (Pedinotti, 2013). Manabe (1969) was the first to include land surface interactions explicitly in

GMDD
8, 2437–2495, 2015

a climate model thorough adopting the simple so-called "Bucket" scheme of Budyko (1961). His scheme predicted the water vapour in the atmosphere, the soil moisture and snow cover without taking into account the soil and vegetation categories. Recent developments in mathematical modelling have been driven primarily by the progress in computer technology, the expansion of modelling into new fields and disciplines and the need for increased accuracy in model predictions (Olchev et al., 2008; Bellocchi et al., 2010). As a result, LSPs have advanced considerably since the simple scheme developed by Manabe (1969) to include detailed parameterisations of momentum, energy, mass and biogeochemistry (Sellers et al., 1997; Rosolem et al., 2013).

One group of LSPs include the Soil–Vegetation–Atmosphere Transfer (SVAT) models. Those are mathematical representations of vertical "views" of the physical mechanisms controlling energy and mass transfers in the soil–vegetation–atmosphere continuum. These deterministic models are able to provide estimates of the time course of soil and vegetation state variables at time-steps compatible with the dynamics of atmospheric processes. During the last number of decades, SVAT models have evolved from simple energy balance parameterisations e.g. the bucket schemes adopted by Manabe (1969), through the schemes of Deardorff (1978), to the Biosphere–Atmosphere Transfer Scheme (BATS) of Dickinson et al. (1986) and the Simple Biosphere (SiB) model of Sellers et al. (1986). Nowadays, they are developed to incorporate complex sub-models including a full integration of connected biogeochemical processes (Sellers et al., 1997; Akkermans et al., 2014). At present, SVAT models are able to describe the multifarious transfer processes through varying degrees of complexity, including the energy, water and carbon dioxide (CO_2) fluxes between the ground surface covered by different vegetation types and the atmosphere over different temporal and spatial scales (Olchev et al., 2008). These embedded modelling efforts require an application context constrained by input variables (atmospheric forcing and vegetation) and input parameters (soil and vegetation properties, initialisation) to simulate the water and energy budget at the surface (Coudert et al., 2008; Ridler et al., 2012).

GMDD
8, 2437–2495, 2015

However, before applying a computer simulation model to perform any kind of analysis or operation, a variety of validatory tests need to be executed. This allows establishing the adequacy of the developed computer model in terms of its ability to reproduce the desired mechanisms with the necessary reality (Petropoulos et al., 2009a). As such, the process of validating a mathematical model's performance, coherence and representation of the natural environment is regarded as an essential step in its development. A comprehensive model validation determines the variance between the model predictions and observations. This allows evaluation of its ability to systematically reproduce the system being simulated (model reliability) and the level of accuracy in which the model reproduces the natural environment (model usefulness) (Huth and Holzworth, 2005; Wallach, 2006). Numerous model validation techniques exist; for a comprehensive overview of validation strategies see Hamilton (1991) and Bellocchi et al. (2010). The procedures to perform the task of validation appear in several forms, depending on data availability, system characteristics and researchers' opinion (Hsu et al., 1999). A common strategy is to examine the model's simulated outputs vs. observations acquired from the real world using common statistical metrics proposed in the classic literature. In addition, Kramer et al. (2002) in an attempt to holistically assess the capability of a model of portraying a real world system, has proposed a set of model assessment criteria, namely: accuracy, generality and realism. Accuracy is described by Kramer et al. (2002) as the "goodness of fit" to in situ measurements. Generality is described as the applicability of the model in numerous ecosystems. Realism is described as the ability of the model to address relationships between modelled phenomena.

The SimSphere land biosphere model is one example of a SVAT model. Formerly known as the Penn-State University Biosphere–Atmosphere Modelling Scheme (PSUBAMS) (Carlson and Boland, 1978; Carlson et al., 1981; Lynn and Carlson, 1990), this 1-D model was considerably modified to its current state by Gillies et al. (1997) and Petropoulos et al. (2013a). Since its early development, the model has become highly variable in its applicational use (for a recent review of the model use see Petropoulos et al., 2009a). Amongst others, it has been involved in studies concerning the study of land surface interactions (Todhunter and Terjung, 1987; Ross and Oke, 1988) and the examination of hypothetical scenarios examining land surface feedbacks (Wilson et al., 1999; Grantz et al., 1999). Furthermore, its use synergistically with Earth Observation (EO) data is being considered at present by several Space Agencies for the development of operational products of energy fluxes and/or soil moisture on a global scale (Chauhan et al., 2003; ESA STSE, 2012). These investigations have been based around the implementation of a technique commonly termed in the literature as the "triangle" (Carlson, 2007; Petropoulos and Carlson, 2011). A variant of it is already deployed over Spain to operationally deliver surface soil moisture at 1 km spatial resolution from ESA's own Soil Moisture and Ocean Salinity (SMOS) satellite (Piles et al., 2011).

As SimSphere's use is rapidly expanding worldwide as both a research and educational tool alike, its validation and establishment of its coherence and correspondence to what it has been built to simulate is of paramount importance. In this respect, a series of Sensitivity Analysis (SA) experiments have already been conducted on the model (Olioso et al., 1996; Petropoulos et al., 2009b, 2013a–c). Such studies have allowed the quantification of the relative influence of each model input to the simulation of key parameters by the model, rank them in order of importance and understand how different parts of the model interplay. Yet, to our knowledge, validation studies involving direct comparisons of model predictions against in situ observations have as of now been scarce and incomprehensive. Such validation exercises have only been performed over a very small range of land use/cover types and on earlier versions of the model when it was still under development (e.g. Todhunter and Terjung, 1987; Ross and Oke, 1988). Furthermore, to our knowledge, very few studies, if any, have acted to specifically validate SimSphere to numerous global ecosystems, for example, over Australian ecosystems. In this context, and given SimSphere's currently expanding global use, a fully inclusive and comprehensive validation of the model is now of fundamental importance.

In this paper, the results from SimSphere's evaluation are presented and its applicability for modelling land surface interactions is demonstrated. The main objective was to understand specifically the models' ability in predicting Shortwave Incoming Radiation (R_g), Net Radiation (R_{net}), Latent Heat (LE), Sensible Heat (H), and Air temperature (T_{air}) at a height of 1.3 and 50 m. Model validation is assessed through a comparison of the model results with corresponding observations from actual in situ measurements acquired at local scale from 8 experimental sites (72 days in total) belonging to the OzFlux (Australia) and AmeriFlux (USA) global monitoring networks. This allowed including contrasting conditions in the model evaluation.

2 SimSphere model description

This work deals with the SimSphere 1-D boundary layer model devoted to the study of energy and mass interactions of the Earth system. It is currently maintained and freely distributed from Aberystwyth University, UK (http://www.aber.ac.uk/simsphere). Figure 1 illustrates the different components of SimSphere's structure, namely the *physical*, the *vertical* and the *horizontal*. Further details about the model architecture can be found in Gillies (1993). In brief, the *physical* components ultimately determine the microclimate conditions in the model and are grouped into three categories, radiative, atmospheric and hydrological. The primary forcing of this component is the available clear sky radiant energy reaching the surface or the plant canopy, calculated as a function of sun and earth geometry, atmospheric transmission factors for scattering and absorption, the atmospheric and surface emissivities and surface (including soil and plant) albedoes.

The *vertical structure* effectively corresponds to the components of the Planetary Boundary Layer (PBL) that are divided into four layers – *a surface mixing layer*, a *surface of constant flux layer*, a *surface of vegetation or bare soil* layer. The depths of all four layers are somewhat variable with time. The top of the mixing layer is identified by the presence of a temperature inversion that caps the air in convective contact with the surface layer. At night, the situation is reversed as the Earth cools down more rapidly than the atmosphere. The surface "constant flux" layer evolves in the model as a series of equilibrium states between the transition layer below and the mixing layer above. Heat and moisture are assumed to be instantaneously conveyed between the surface and the top of the surface layer, which is chosen to be at a height of 50 m. In reality this height varies between 20 and 50 m. The transition layer applies to a layer in which the vertical exchanges are dominated by molecular and radiative effects as well as by vertical wind changes. In the case of vegetation, the transition layer is represented by the microclimate within and at the top of the vegetation canopy. The substrate layer refers to the depth of the soil over which heat and water is conducted. It consists of two layers, a surface layer and a root zone. Water flows from the surface and the root zone to the atmosphere respectively by direct evaporation or through the plants as well as between the two layers. Soil water content is specified by assigning a fractional volume of field capacity, which essentially is the "soil moisture availability". Five layers are used to compute the flow of heat in the substrate. An initial soil temperature profile is assigned on the basis of the initial surface temperature (furnished from a meteorological sounding) and a climatological substrate temperature, which one obtains from mean data. A governing parameter for heat conduction is the "thermal inertia" that contains both soil conductivity and soil diffusivity (or alternately, the volumetric heat content). This parameter is the one that also governs the rate of H flux to or from the atmosphere through the soil surface.

The *horizontal* component of the model is composed of 4 parts: (i) *Planetary Boundary Layer* (PBL), (ii) *Surface Layer*, (iii) *Transition Layer* and (iv) *Substrate Layer*. Due to SimSphere simulating parameters in a 1-dimensional vertical column, the model is restricted horizontally only to areas representative of its initialised conditions, therefore the model has an undefined spatial coverage. The vegetation component is dormant at night, that is, after radiation sunset. The night time dynamics for the surface fluxes differ from those during the day time. Heat and moisture fluxes are exchanged between both the ground and foliage, between plant and inter-plant airspaces through stomatal and cuticular resistances in the leaf (for water vapour) and the air, between soil and the interplant air spaces and between the entire vegetation canopy and the air. A separate component exists for the bare soil fluxes between the surface and the air. Vegetation and soil fluxes meld at the top of the vegetation canopy, their relative weights depending on the fractional vegetation cover, which is specified as an input to the model. As such, SimSphere is thus referred to as a form of two-stream or two-source model. The soil hydraulic parameters are prescribed from the Clapp and Hornberger (1978) classification. The soil surface turbulent fluxes are determined following the Monin and Obukov (1954) similarity theory which takes into account atmospheric stability.

SimSphere represents various physical processes taking place in a column that extends from the root zone below the soil surface up to a level well above the surface canopy, the top of the surface mixing layer. The processes and interactions simulated by the model are allowed to develop over a 24 h cycle at a chosen time step (typically 30′), starting from a set of initial conditions given in the early morning. For its parameterisation, input parameters are categorised into 7 defined groups; time and location, vegetation, surface, hydrological, meteorological, soil and atmospheric (Table 1). From initialisation, over a 24 h cycle SimSphere assesses the diurnal evolution of more than 30 prognostic variables associated with the radiative, hydrological and atmospheric physical domains. Outputs of the model include, between others, the surface energy fluxes (LE and H fluxes) below and at the soil surface, around and above the vegetation canopy and the transfer of water in the soil and in the plants. Several meteorological parameters are also predicted including the radiometric surface temperature, wind velocity, air temperature, and humidity at various levels in and above the canopy.

3 Experimental set up

A total of 5 AmeriFlux and 3 OzFlux experimental sites were used, providing a comprehensive dataset of measured micrometeorological parameters together with general meteorological observations. Both networks are part of FLUXNET, the largest global network of micrometeorological flux measurement sites. The flux sites use eddy covariance methods to measure the exchanges of carbon dioxide, water vapour, and energy between terrestrial ecosystems and the atmosphere (Aubinet et al., 2000). Table 2 provides an overview of the experimental sites characteristics used in this study, whereas the geographical location of those sites within USA and Australia is illustrated in Fig. 2. At each site, micrometeorological measurements of various parameters are acquired, including the turbulent fluxes of heat and moisture, Shortwave Incoming Radiation (R_g), Net Radiation (R_{net}) and Air Temperature (T_{air}) (often at different heights). Flux measurements methods and calculations performed within the FLUXNET sites are designed with the same hardware and software specifications at all sites. All data are quality-controlled and standard procedures for error corrections are prescribed. Details on the FLUXNET measurements and the processing of the raw data can be found in Aubinet et al. (2000).

The sites included in this study to validate SimSphere were representative of a range of ecosystem types with markedly different site characteristics to include contrasting conditions in the model evaluation. All in situ data acquired from each site was collected covering the year 2011, allowing for a sufficient database for model parameterisation and validation to be developed. All data was obtained from the FLUXNET database (http://fluxnet.ornl.gov/obtain-data) at both Level 2 (AmeriFlux) and Level 3 (OzFlux) processing levels. At both processing levels, the data has been subjected to basic quality control checks with the removal of erroneous data, and has also been subject to quality control and post processing (for the case of level 3 data). For both networks, no gap filled data was used to ensure that modelled predictions were compared against actual observational measurements as opposed to estimated values. Additionally, atmospheric in situ data was collected from the freely distributed University of Wyoming's weather balloon data archive (http://weather.uwyo.edu/upperair/sounding.html). Local profiles of temperature, dew point temperature, wind direction, wind speed and atmospheric pressure were taken from nearest possible experimental sites which and were also used in model parameterisation.

4 SimSphere parameterisation and validation

This section provides a synopsis of the methodology followed in evaluating SimSphere's ability to simulate key parameters characterising land surface interactions. An overview of the main steps included in this process is furnished in Fig. 3.

4.1 Datasets pre-processing

Following data acquisition, further analysis was implemented aimed at identifying the specific days for which SimSphere would be parameterised and validated for each experimental site. Initially, cloudy days were identified and eliminated from any further analysis. Judgement on which days (or time-periods) were cloud-free was based on the observation of R_g diurnal observation, where cloud-free days were flagged as those having smooth and symmetrical R_g curves, a property signifying clear-sky conditions (e.g. Carlson et al., 1991).

Subsequently, for the subset of cloud-free days, the Energy Balance Closure (EBC) was evaluated. EBC evaluation has been accepted as a valid method for accuracy assessment of turbulent fluxes derived from eddy covariance measurements (Wilson et al., 2002; Barr et al., 2006). Energy imbalance provides important information on how they should be compared with model simulations (e.g. Twine et al., 2000; Culf et al., 2002). In this study, EBC was principally evaluated by performing a regression analysis (e.g. see Wilson and Baldocchi, 2000; Wilson et al., 2002; Castellvi et al., 2006). The linear regression coefficients (slope and intercept) as well as the coefficient of determination (R^2) were calculated from the Ordinary Least Squares (OLS) relationship between the 30 min estimates of the dependent flux variables (LE + H) and the independently derived available energy ($R_{net} - G - S$). In addition to this, the Energy Balance Ratio (EBR) parameter was computed by cumulatively summing $R_{net} - G - S$ and LE + H from the 30 min mean average surface energy flux components, and then rationing each of the cumulative sums as follows (e.g. Wilson et al., 2002 ; Liu et al., 2006):

$$\mathrm{EBR} = \frac{\sum(\mathrm{LE} + H)}{\sum(R_{\mathrm{net}} - G - S)} \quad (1)$$

This index generally ranges from zero to one, with values closer to one highlighting a satisfactory diurnal energy closure, indicating a good quality of in situ measurements. All days with poor EBC ($\mathrm{EBR} < 0.75$, $\mathrm{slope} < 0.85$, $R^2 < 0.930$) were excluded from further analysis.

Further conditions were subsequently employed to ensure that selected days were of the highest possible quality in terms of in situ data quality. Firstly, all days selected were within the same year to eliminate effects ascribed from inter-annual variability in vegetation phenology or climatic conditions. Secondly, selected simulation days were assessed for atmospheric stable conditions, namely low wind speeds and low available energy (Maayar et al., 2001). Such conditions were identified by the evaluation of the in situ data, where direct measurements of wind speed and energy flux amplitude and diurnal trend were used as indicators of atmospherically stable conditions. As a result, a final set of a total of 72 non-consecutive days from the different experimental sites were identified as being suitable for use in SimSphere validation.

4.2 Model parameterisation

SimSphere was parameterised to the daily conditions existent at the flux tower for each of the selected days. In situ data sets provided measurements of soil water content, temperature, wind speed, wind direction and atmospheric pressure at the corresponding time of initialisation, 06:00 LT. Ancillary parameters, critical for the models' initialisation, were largely acquired through either the sites respective Principal Investigator (PI) (for the case of OzFlux), or the FLUXNET database (for the case of AmeriFlux). Such measurements included detailed information on the vegetation (LAI, FVC, vegetation height, cuticle resistance), pedological (soil morphology and soil classification) and topographical (slope, aspect, surface roughness) characteristics of each site. If no ancillary information was available, specific parameters were acquired through the analysis of standard literature sources (e.g. Mascart et al., 1991; Carlson et al., 1991). The soil type parameters were obtained using the soil texture data provided at each FLUXNET test site and information supplied in some instances by the experimental site managers themselves. This was also the case for the topographical information required in model initialisation. Wind and water vapour sounding profiles which were attained at 06:00 GMT from the University of Wyoming database to correspond to the models' initialisation were also used in model parameterisation. Upon completion of its initialisation, the model was executed for each site/day forced by observations acquired from each site on which it had been parameterised. The 30′ average value of each of the targeted model outputs per site for the period 05:30–23:30 LT was subsequently exported in SPSS to validate the model predictions.

4.3 Model performance assessment

Due to a good database of reference data from the OzFlux and AmeriFlux networks, a multi-faceted validation of the model was feasible. The two datasets were compared using a series of statistical terms which included the Mean Bias Error (MBE, or bias – Eq. 2) and Mean Standard Deviation (MSD, or scatter – Eq. 3) of the observed and modelled values, the Root Mean Square Difference (RMSD) (Eq. 4), the Mean Absolute Difference (MAD) (Eq. 5) the linear regression fit model coefficient of determination (R^2) (Eq. 6) and the Nash–Sutcliffe (1970) (denoted as Nash) index (Eq. 7):

$$\text{Bias} = \text{MBE} = \frac{1}{N}\sum_{i=1}^{N}(P_i - O_i) \tag{2}$$

$$\text{Scatter} = \text{MSD} = \frac{1}{(N-1)}\sum_{i=1}^{N}\left(P_i - O_i - \overline{(P_i - O_i)}\right)^2 \tag{3}$$

$$\text{RMSD} = \sqrt{\text{bias}^2 + \text{scatter}^2} \tag{4}$$

GMDD
8, 2437–2495, 2015

Validating a 1-D SVAT model

G. P. Petropoulos et al.

Title Page
Abstract Introduction
Conclusions References
Tables Figures
◀◀ ▶▶
◀ ▶
Back Close
Full Screen / Esc
Printer-friendly Version
Interactive Discussion

$$\mathrm{MAD} = N^{-1}\sum_{i=1}^{N}|P_i - O_i| \tag{5}$$

$$R^2 = \left[\sum_{i=1}^{N}\left(P_i - \overline{P}\right)\left(O_i - \overline{O}\right) \Big/ \left[\sum_{i=1}^{N}(O_i - \overline{O})^2 \sum_{i=1}^{N}\left(P_i - \overline{O}\right)^2\right]^{0.5}\right]^2 \tag{6}$$

$$\mathrm{NASH} = 1 - \left[\frac{\sum_{i=1}^{N}(O_i - P_i)^2}{\sum_{i=1}^{N}(O_i - \overline{O})^2}\right] \tag{7}$$

P denotes the "predicted" values obtained from SimSphere and O denotes the "observed" values from the selected OzFlux and AmeriFlux site-days.

The utilisation of these statistics to characterise the quality of model simulations has been widely demonstrated in a number of previous studies comparing model outputs to observational networks (e.g. Alexandris and Kerkides, 2003; Marshall et al., 2013). All statistical metrics were computed from comparisons performed at identical 0.5 hourly intervals between the two datasets for each day of comparison. In addition, these statistical parameters, where appropriate, were also computed for each site, providing a summary of the model predictions per experimental site.

5 Results

The main results from the SimSphere validation for each of the model predicted parameters evaluated in this study are summarised in Tables 3 to 8. In addition, Figs. 4 to 9 provide a graphical illustration in the form of a scatterplot of the agreement between the simulated values and in situ measurements per parameter for all sites together. The detailed validation of the model performance is provided next.

GMDD
8, 2437–2495, 2015

5.1 Incoming shortwave radiation (R_g)

Simulation accuracy of R_g was largely accurate, exhibited by low RMSD and MAE values, and also high correlation coefficients (RMSD = 67.83 W m^{-2}, MAE = 46.43 W m^{-2}, R^2 = 0.97, NASH = 0.963) (Table 3 and Fig. 4). A moderate underestimation of the observed fluxes was also evident (MBE = −19.48 W m^{-2}). Although simulation accuracies were generally satisfactory, it should be noted that simulation of R_g by the model displayed both the highest mean error (RMSD = 67.83 W m^{-2}, MAE = 46.43 W m^{-2}), and also the highest variable range of RMSD on a per site basis of all the parameters (39.97 to 100.65 W m^{-2}). MSD similarly displayed a high range of values (36.57 to 83.36 W m^{-2}) when evaluated on a per site basis, showing to some extent a deficiency in the capability of the model to fully capture the land surface process. Notably, in contrast, R_g also yielded highest correlated results of all parameters assessed (R^2 = 0.971). This was further illustrated in Fig. 4, where the distribution of points was mainly centred on the 1 : 1 line.

When analysing the results on a per site basis, the highest simulation accuracies were attained within the US_MOZ deciduous broadleaf site in comparison to all other sites (MSD = 47.58 W m^{-2}, RMSD = 50.36 W m^{-2}, MAE = 36.57 W m^{-2}, R^2 = 0.981). However, the Howard Springs woody savannah site also attained comparable high simulation accuracies (MBE = 50.37 W m^{-2}, RMSD = 52.53 W m^{-2}, MAE = 33.79 W m^{-2}, R^2 = 0.981). The model predictions of R_g for the US_WHS shrubland site was significantly lower, indicating weakest model performance within this site (RMSD = 100.65 W m^{-2}, R^2 = 0.964, MBE = −56.40 W m^{-2}, MSD = 83.36 W m^{-2}), closely followed by the Australian Calperum grazing pasture site (RMSD = 90.45 W m^{-2}, R^2 = 0.956, MBE = −40.42 W m^{-2}, MSD = 80.91 W m^{-2}). Within the majority of sites, model simulation consistently underestimated the in situ measurements (MBE = −4.85 W m^{-2} to 56.40 W m^{-2}), with the US_MOZ deciduous forest site being the only exception (MBE = 16.47 W m^{-2}).

GMDD
8, 2437–2495, 2015

Evidently, accuracy of model estimations over the Australian sites generally increased for the period between February to June, with a significant decrease in accuracy from August to early February. For example, over the Calperum grazing pasture site, RMSD ranged from 24.14 to 53.78 $W m^{-2}$ for all the test days located within the period from 24 February 2011 to 24 April 2011. In contrast, for the same site, RMSD varied from 84.41 to 149.29 $W m^{-2}$ for all the test days within the period between 22 July 2011 to 29 December 2011. Similar trends were observed for all other Australian sites, although some anomalies were present. In relation to the US sites the adverse was found; highest simulation accuracy were predominantly derived for the test days located during the period between October and late April. Generally the results for the US sites suggested that the conditions prevalent within the wet season (October to May) may have had an influence on model accuracy.

5.2 Net radiation (R_{net})

Table 4 and Fig. 5 indicate a high overall performance in the models' ability to accurately predict R_{net}, confirmed by the high simulation accuracy (RMSD = 58.69 $W m^{-2}$, MAE = 46.42 $W m^{-2}$ and R^2 = 0.96) reported for all sites. Furthermore, comparisons of R_{net} for all days of simulation showed an average MSD of 54.44 $W m^{-2}$, indicating the model's capability to precisely represent the amplitude of the R_{net} flux, with low dispersion of variance from the in situ trends. This is also evidenced in Fig. 5 where the points within the scatterplot are closely distributed on the 1 : 1 line. MBE results indicated a moderate underestimation of the in situ measurements by the model (−16.49 $W m^{-2}$). The R_{net} results exhibited largely similar statistical agreement to those observed for those of the R_g parameter.

Most noticeably, in correspondence with the R_g parameter results, the model showed superior simulation accuracy within the Alice Springs mulga woodland site in comparison to the other land cover types, with the reported accuracies significantly above the overall average (RMSD = 33.90 $W m^{-2}$, R^2 = 0.988, MBE = −16.35 $W m^{-2}$,

$\mathrm{MSD} = 29.69\,\mathrm{W\,m^{-2}}$, $\mathrm{MAE} = 26.25\,\mathrm{W\,m^{-2}}$, $\mathrm{NASH} = 0.981$). Moreover, the woody savannah site of Howard Springs again also exhibited high simulation accuracies ($\mathrm{RMSD} = 47.05\,\mathrm{W\,m^{-2}}$, $R^2 = 0.974$, $\mathrm{MBE} = 10.35\,\mathrm{W\,m^{-2}}$, $\mathrm{MSD} = 45.89\,\mathrm{W\,m^{-2}}$, $\mathrm{MAE} = 35.74\,\mathrm{W\,m^{-2}}$, $\mathrm{NASH} = 0.972$). Conversely, the model showed an inferior performance when simulating R_{net} within the US_TON wooded savannah site. A systematic underestimations of R_{net} was evident, leading to an overall satisfactory agreement between the model predictions and in situ observations ($\mathrm{RMSD} = 78.03\,\mathrm{W\,m^{-2}}$, $R^2 = 0.954$, $\mathrm{MBE} = -46.10\,\mathrm{W\,m^{-2}}$, $\mathrm{MSD} = 62.96\,\mathrm{W\,m^{-2}}$). It should be noted that the accuracy of the model estimations on a per site basis did not correlate between both the R_g and R_{net} parameter estimations, with only the US_WHS shrubland site exhibiting weaker simulation accuracies for both parameters. Notably, Howard Springs, an open wooded savannah ecosystem, was the only site on which an overall overestimation of the in situ measurements by the model was reported ($\mathrm{MBE} = 10.35\,\mathrm{W\,m^{-2}}$). For all other sites the model systematically underestimated R_{net} with negative MBE values in a range of -0.09 to $-46.10\,\mathrm{W\,m^{-2}}$.

Evidently, as indicated by Table 4, trends in simulation accuracy dependent on test day were apparent. Although comparable; the trends were not as prominent as those exhibited for the R_{net} parameter. Within the Australian sites, low RMSD was exhibited predominantly for the test days within the period of March to July, although some discrepancies were present during specific days. For example, the date of 23 March 2011 for the Alice Springs site indicated an RMSD of $62.14\,\mathrm{W\,m^{-2}}$, with the 27 May 2011 simulation date for the Howard Springs site indicating an RMSD of $70.60\,\mathrm{W\,m^{-2}}$. However, such anomalies were limited. Generally, for the US sites, highest RMSD was exhibited for the period concurrent to the wet season (October to April), with the highest error for a specific date exhibited for the 27 February 2011 US_IB1 site ($\mathrm{RMSD} = 113.80\,\mathrm{W\,m^{-2}}$), although again, anomalies in such trends were notable yet uncommon.

5.3 Latent heat (LE)

As presented in Table 5, lowest RMSD was reported for the LE parameter in comparison to all other parameters evaluated (RMSD = 39.47 W m^{-2}). This appraises the models' ability to accurately reproduce LE fluxes in numerous global ecosystems, both in terms of their seasonal and diurnal evolution. However, an average R^2 value of 0.700 suggests a weaker representation of the LE trend in comparison to all other parameters, see Fig. 6. When averaged over all days and sites, LE was slightly overestimated; this is reported by an average MBE of 2.84 W m^{-2}. However, this result was insignificant, indicating the models' capability to accurately report the trends in LE flux amplitude. Alongside this, the MSD values reported for LE were significantly lower than those reported for the R_{net}, H and R_{g} parameters.

The model showed excellent precision in reproducing daily trends of LE fluxes in most sites evaluated; this was evidenced for example by the low overall MSD value of 37.87 W m^{-2} which was significantly lower than all other fluxes analysed in the present study. When analysed on a site by site basis, in correspondence with the R_{net} parameter results, the Alice Springs mulga woodland site consistently yielded the highest statistical agreement between model predicted and observed values, with low error and high correlation results (RMSD = 24.75 W m^{-2}, R^2 = 0.827, MBE = 2.75 W m^{-2}, MSD = 24.59 W m^{-2}, MAE = 15.16 W m^{-2}, NASH = 0.945). Notably, the US-Whs shrubland site also exhibited comparably high accuracy. This was in contrast to the weaker agreement displayed for this site between the estimated and measured values for the R_{g} and R_{net} modelled parameters. Moreover, the deciduous broadleaf forest site, US_MOZ, which exhibited greatest simulation accuracy for the R_{g} parameter, yielded less satisfactory simulation accuracy in comparison to all other sites (RMSD = 61.52 W m^{-2}, MAE = 42.02 W m^{-2}), with values exhibiting a high average MSD (55.92 W m^{-2}) and a general overestimation of LE (MBE = 22.65 W m^{-2}). Similar high MSD values were reported in the Howard Springs woody savannah site (MSD = 50.06 W m^{-2}) and the US_IB1 cropland site (MSD = 52.47 W m^{-2}). Generally, each site exhibited a significant range of MBE, from −11.49 $\mathrm{W\,m^{-2}}$ (US_WHS) to 25.65 $\mathrm{W\,m^{-2}}$ (US_MOZ), suggesting high variability between the partitioning of LE in each ecosystem. Peak LE flux values exhibited high inter-site variability, with both the US_IB1 (cropland) and US_MOZ (deciduous broadleaf forest) sites containing the highest LE flux peaks of 458.5 and 376 $\mathrm{W\,m^{-2}}$ respectively. In comparison, a maximum LE flux peak of just 143.7 $\mathrm{W\,m^{-2}}$ was reported for the US_WHS (Shrubland) site, suggesting a substantial range of 314.8 $\mathrm{W\,m^{-2}}$ between lowest daily and maximum daily LE peak. Noticeably, trends in simulation accuracy dependent on test day were comparable to both the R_g and R_{net} parameter results, yet with lower inter-site variability in RMSD ranges.

5.4 Sensible heat (H)

SimSphere consistently showed a high ability to accurately simulate H fluxes in numerous ecosystems globally, with an average RMSD and R^2 values of 55.06 $\mathrm{W\,m^{-2}}$ and 0.829 respectively. Results were largely similar to that of the LE flux simulation accuracies, although model performance for the LE parameter outperformed that of the H flux for the majority of statistical metrics computed herein.

Average RMSD values ranged from 38.07 to 69.94 $\mathrm{W\,m^{2}}$ (US_VAR and US_WHS) when analysed on a site by site basis. In addition, R^2 values ranged from 0.73 (US_IB1) to 0.94 (US_VAR). The latter was suggestive that model predictions were in good to excellent agreement to the in situ measurements. The grassland site (US_VAR) consistently showed superior model performance in comparison to all other sites, with values indicating an excellent agreement to the observed diurnal evolution (RMSD = 38.07 $\mathrm{W\,m^{-2}}$, R^2 = 0.941, MBE = 13.82 $\mathrm{W\,m^{-2}}$, MSD = 33.48 $\mathrm{W\,m^{-2}}$, MAE = 28.35 $\mathrm{W\,m^{-2}}$, NASH = 0.930). MSD values reported for US_VAR were 19.41 $\mathrm{W\,m^{-2}}$ lower than the all site average, suggesting a systematically accurate representation of H at this site. MSD values reported for H flux were directly comparable to the overall average MSD values reported for R_g and R_{net}, but were significantly higher than those reported for the LE parameter. Accuracy ranges for the simulated H fluxes for all other sites exhibited comparable ranges (RMSD = 50.39–69.94 $W m^{-2}$). SimSphere was often unable to represent the peak of H fluxes across all sites; this is shown by the MSD of values represented in Fig. 7, which is most noticeable over the US_WHS site where SimSphere showed inferior performance in simulating H flux trend and magnitude in comparison to all other sites. Results for the US_WHS site thus exhibited poor RMSD and MSD values (69.94 and 67.73 $W m^{-2}$ respectively), adverse to the high accuracies reported over this site for the LE parameter. In addition to this, the US_IB1 (cropland) and US_MOZ (deciduous broadleaf forest) sites demonstrated a significantly lower flux magnitude than other sites, with peak H flux values of just 307 and 278 $W m^{-2}$ respectively. These peak fluxes were significantly lower compared to that of US_WHS (shrubland) which had a peak H flux magnitude of 481 $W m^{-2}$.

The trends in inter-site variability of RMSD dependent on simulation day were significantly less apparent for the H flux results in comparison to the three previous parameters (R_g, R_{net} and LE). For the Australian sites, no significant trends were evident, with generally comparable accuracy ranges for the specific test days including anomalistic days which exhibited significantly higher error ranges. For example, the Howard Springs woody savannah site indicated RMSD for the majority of simulation days ranging between 28.29 and 50.31 $W m^{-2}$ on a per test day basis, with the 13 April 2011 and 13 May 2011 days exhibiting an RMSD of 75.86 and 96.93 $W m^{-2}$ respectively. Similar inter-site variability was notable for the US sites.

5.5 Air temperature 1.3 m ($T_{air\ 1.3\ m}$)

SimSphere showed a high capability in simulating $T_{air\ 1.3\ m}$ with an average RMSD as low as 3.23 °C and relatively high R^2 value of 0.843, see Table 7. Furthermore, $T_{air\ 1.3\ m}$ exhibited neither a consistent over or underestimation, with an overall average MBE of 0.28 °C. Simulation accuracy for $T_{air\ 1.3\ m}$ was relatively stable, with a low range of RMSD values reported over all sites. RMSD values ranged from 2.17 °C in the woodland savannah site of Howard Springs, and 4.74 °C in the grazing pasture site of Calperum. Overall, agreement between the predictions and observations was greatest for the Howard springs site, with results confirming a high overall correlation to the observed diurnal evolution of $T_{air\,1.3\,m}$ (RMSD = 2.17 °C, R^2 = 0.792, MBE = 0.56 °C, MSD = 2.10 °C, MAE = 1.84 °C, NASH = 0.853). The deciduous broadleaf site of US_MOZ also exhibited comparably high simulation accuracy (RMSD = 2.38 °C, R^2 = 0.928, MBE = 0.23 °C, MSD = 2.37 °C, MAE = 1.84 °C, NASH = 0.853). The Calperum site exhibited the weakest agreement of $T_{air\,1.3\,m}$ with an average RMSD 1.51 °C higher than the all site average. The R^2 analysis further appraised the models ability to accurately simulate air temperature, with a range of values indicating high correlation between model predicted and observed $T_{air\,1.3\,m}$ (0.74 to 0.93). MSD displayed a high range of values (2.1 to 3.76 °C), showing to some extent the inability of the model to consistently predict $T_{air\,1.3\,m}$ with a high level of precision. The trends in simulation accuracy dependent on test day were again insignificant for the $T_{air\,1.3\,m}$ parameter, exhibiting similar patterns to those indicated for the H flux parameter.

5.6 Air temperature 50 m ($T_{air\,50\,m}$)

As illustrated in Table 8 and Fig. 9, the model showed a slightly inferior performance in predicting $T_{air\,50\,m}$ (RMSD = 3.77 °C) when compared to $T_{air\,1.3\,m}$ (RMSD = 3.23 °C), with an average RMSD difference of 0.54 °C. A decrease in correlation between the predicted and observed values was also evident between both parameters, with a lower average R^2 value of 0.775 compared to that of $T_{air\,1.3\,m}$ (R^2 = 0.843). However, the values reported still showed a highly acceptable correlation between the modelled estimates and the in situ measurements, as indicated by an average NASH value of 0.825. Once averaged, $T_{air\,50\,m}$ exhibited a minor underestimation of −0.38 °C; however the range of MBE reported between sites was significantly less (2.1 °C), suggesting a more consistent simulation of T_{air} at 50 m compared to at 1.3 m by SimSphere. In contrast, agreement between the simulated $T_{air\,50\,m}$ and in situ measurements resulted

GMDD
8, 2437–2495, 2015

in a higher MSD than that reported for the $T_{\text{air 1.3 m}}$ parameter, with the exception of the Howard Springs site. When analysed on a per site basis, notably, in correspondence with the $T_{\text{air 1.3 m}}$ parameter, agreement between the estimated and measured values over both the Howard Springs and US_MOZ sites exhibited highest simulation accuracy (RMSD = 2.04 and 2.85 °C respectively). Moreover, weakest agreement was reported over the Calperum site, again in correspondence with the results of the $T_{\text{air 1.3 m}}$ parameter. No systematic trends were apparent in the inter-site variability of simulation accuracy dependent on test day.

6 Discussion

In this study the ability of the SimSphere SVAT model to accurately represent various heat and water exchanges within different global ecosystems was evaluated. A total of 72 days from year 2011 were selected from Australia and USA to validate the model's ability to predict Shortwave Incoming Radiation (R_g), Net Radiation (R_{net}), Latent Heat (LE), Sensible Heat (H), and Air temperature (T_{air}) at a height of 1.3 and 50 m.

In overall, the model proved capable in predicting the diurnal variation of all parameters to a satisfactory level of accuracy. In particular, SimSphere demonstrated a promising ability to accurately simulate LE and H within all ecosystems, indicated by relatively high correlation values and low average prediction error for both parameters (Tables 6 and 7). Variable model performance was clearly evident when simulating both the LE and H fluxes within contrasting land cover types. For example, as discussed, highest simulation accuracy was attained within the grassland study sites. In contrast, simulation accuracy within forested ecosystems was less satisfactory. The deciduous forest stand (US_MOZ), with an average canopy height of 24.2 m, attained low simulation accuracy, and was outperformed by the mulga forested ecosystem (Alice Springs), characterised by a sparse canopy at a height of 6.5 m. Such results suggest that the increased complexity and heterogeneity of forested environments, particularly those with understory vegetation, can have profound effects on the overall exchange of mass and energy which cannot be represented within the models parameterisation and hence can influence LE and H outputs. The partitioning of LE and H fluxes are also highly susceptible to a number of other factors. Small changes in the moisture availability, most particularly from the deep layer soil water content (SWC), can have a strong influence on the partitioning of the fluxes (Carlson and Lynn, 1991; Olioso et al., 2000), but also on the representativeness of the radiosonde data to the existent local conditions (Taconet et al., 1986). Taconet et al. (1986) found that an error of just $\sim 2\,^{\circ}\mathrm{C}$ in the sounding profile temperature can cause a variation of $\sim 45\,\mathrm{W\,m^{-2}}$ in the corresponding fluxes, most particularly so for H flux. As SimSphere was forced with surface moisture and root zone moisture availability data taken directly from the in situ data, as well as nearby representative sounding profiles, an accurate representation of the local conditions were attained. These highly influential parameters were thus consistently represented within the models' parameterisation, providing a possible reason in part for the high simulation accuracies attained.

R_g was estimated by the model to a satisfactory level of accuracy, however overall, simulation accuracy was the weakest of all parameters evaluated (mean RMSD = $67.82\,\mathrm{W\,m^{-2}}$). The weaker performance of the model in simulating this parameter can potentially be attributed to the variations in the soil temperature and moisture which has an indirect impact on R_g (Cui et al., 2009). However, a high R^2 value of 0.971 reported for all days of analysis suggests that model predictions had excellent correlation to the observed dataset. This indicates that SimSphere was able to simulate the trend of R_g well, but not necessarily the amplitude. A possible reason for the underestimation of R_g by the model is perhaps linked to the solar transmission model and/or the surface albedo calculation in the model, as has also been pointed out previously by Todhunter and Terjung (1978). Furthermore, previous sensitivity analysis studies undertaken upon the model confirm that R_g is significantly influenced by the sites aspect (Petropoulos et al., 2014). Therefore the lower simulation accuracy reported may partly be related to misrepresentation of the sites topographical characteristics. In the majority of the experimental sites a general underestimation of R_{net} was attained by

GMDD
8, 2437–2495, 2015

the model, which led to a mean RMSD and R^2 value of 58.69 $\mathrm{W\,m^{-2}}$ and 0.96 respectively. These results are also comparable to those reported in other analogous validation studies (Carlson and Boland, 1978; Todhunter and Terjung, 1987; Ross and Oke, 1988). Todhunter and Terjung (1987) compared predicted R_{net} from the model vs. corresponding R_{net} values obtained from the literature from Los Angeles, USA, and showed both daytime and night time simulations to be in agreement within the range reported in the literature. Ross and Oke (1988) also confirmed the capability of the model in simulating the day-to-day variation of R_{net} for comparisons using eighteen cloud-free days over an urban area of Vancouver, B.C. in Canada. They reported an overall average RMSD error of 43 $\mathrm{W\,m^{-2}}$ for comparisons of all cloud-free days, a minor improvement on the RMSD of 58.69 $\mathrm{W\,m^{-2}}$ presented herein. Disparity in the results between this work and those studies could be the results of utilising model simulations over dissimilar land cover types, where it is largely accepted that R_{net} partitioning into LE and H fluxes is highly dependable on the vegetation and surface characteristics of the site (Olioso et al., 2000). Previous sensitivity analysis studies undertaken on SimSphere further confirm this observation (Petropoulos et al., 2014). Similarly to R_g, simulation accuracy of R_{net} was described by Ross and Oke (1988) to be a factor of long wave radiation, mainly the values of atmospheric and surface emissivities (which effect the surface temperature estimation). Increased representation of the surface optical properties and long wave radiation estimation of the model could greatly enhance simulation accuracy.

Overall simulation accuracies were lower for estimates of $T_{air\,50\,m}$ compared to estimates of $T_{air\,1.3\,m}$ in all but one site, Howard Springs. One possible explanation for this may be the fundamental problem that model estimates of $T_{air\,50\,m}$ could only be validated against ancillary air temperature data obtained directly from the sites flux tower, thus direct comparison specifically at 50 m could not be achieved. Similarly to the LE and H fluxes, variable simulation accuracies dependent on land cover types were also evident. Three sites: Calperum, US_VAR and US_IB1, all exhibit noticeably weaker simulation accuracies in comparison to the remaining sites. On further investigation,

GMDD
8, 2437–2495, 2015
Validating a 1-D SVAT model
G. P. Petropoulos et al.

all 3 sites show an ecosystem which is characterised by high inter-annual variability of vegetation phenology, such as vegetation height, leaf width, FVC etc. Modelled T_{air} peaked between 10:30 and 14:30 LT, displaying a slight lag in comparison to the in situ observations on some occasions. In instances where time-lag between the predicted and observed T_{air} comparisons is observed, such effects may be linked with the energy storage in the vegetation and the air, something which is not taken into account in the SimSphere simulations. This may partly explain some of the inaccuracies reported for T_{air} estimation in Alice Springs and US_MOZ as this effect is most important for forested sites. Carlson and Boland (1978) and Carlson et al. (1991) also described a similar "hysteresis" effect in comparisons which they performed for different vegetation canopies and environmental conditions (urban and rural environments). Carlson and Boland (1978) suggested thermal inertia to be related proportionally to an increase in the time lag between solar noon and the time of maximum H flux and T_s, whereas Carlson et al. (1991) admitted that they were unable to practically explain this "hysteresis" trend. Through comprehensive sensitivity analysis studies undertaken by Petropoulos et al. (2009b, 2013a–c, 2014), parameters closely associated to vegetation phenology have been previously outlined to have a highly influential control on air temperature magnitude and extent. Conversely, sites which show relatively stable vegetation phenology such as US_TON (wooded savannah) exhibited more accurate temperature estimates. Furthermore, the air temperature of the site covered by the dead forest had greater daily fluctuation compared to the stands covered by mature forest which generally had the smallest daily fluctuations. However, more studies are required in this direction in categorising the dead forest from mature forest, which is currently not possible in the given land cover database. As the SimSphere model assumes a homogenous canopy layer, some discrepancies may also occur in the air temperature simulation, which seemed to be the case in the present study. Furthermore a very important point to consider in the overall interpretation of the results is that the model does not account for advective conditions which may be important when strong winds exist. Yet generally, the results obtained showied a significant improvement on values reported in previous validation attempts (Carlson and Boland, 1978; Carlson et al., 1991), suggesting that air temperature at 1.3 and 50 m was well represented by the model.

All in all, SimSphere demonstrated a high capability of simulating parameters associated with the Earth's energy balance. It is also apparent that the model fulfils 3 of Kramer et al.'s (2002) model assessment criteria, *namely accuracy, generality and realism* (see also Sect. 1). In regards to accuracy, no significant systematic prediction errors occurred within all of the fluxes analysed, with the exception of a consistent underestimation of R_{net}. Additionally, simulated peak heat and water flux values were in high accordance with the in situ data, typically at 12:30–13:30 LST, with a slight lag for LE and H fluxes (13:00–14:00 LST). In terms of *generality*, the model has shown high levels of generality, with acceptable simulation accuracies attained in all sites validated. In order to improve the models generality, the inclusion of more forested environments would comprehensively assess the models applicability to different land cover types, particularly heterogeneous forest stands where simulation accuracy tends to be lower. Finally, *realism* in the model has been most notable in the simulation of LE, H and T_{air} fluxes, where slight change in the vegetation phenology or SWC was accountable for characterising the diurnal evolution of fluxes in all sites validated.

The study conducted herein can advance our understanding of SimSphere's ability to simulate interactions between different components of the Earth system and related land surface processes. As no model is perfect some discrepancies between model predictions and measurements will always appear. Identification of these discrepancies are most interesting, because they can teach us more about causes of model uncertainties in the prediction of hydro-meteorological variables, and help us improve the model structure and performance. Some large discrepancies between the simulated and observed datasets could be due to model parameterisation. Apart from environmental factors, tower flux instrumentation error, indicated by the presence of spike (too large or too small values) measurements in the datasets, can also affect the accuracy, even if model simulated results are in agreement with actual conditions. The

GMDD
8, 2437–2495, 2015

other possible reasons is the presence of spikes in the fluxes, observed particularly on the days of low agreement, which could have occurred from horizontal advection, footprint changes as well as a non-stationarity of turbulent regimes (Papale et al., 2006). Unfortunately, such conditions cannot be captured and replicated by SimSphere.

In overall, it is important to recognise that uncertainty is inevitable in any model as it will never be as complex as the reality it portrays. Thus, the model fulfills its objective as a tool to accurately monitor and simulate land surface interactions. It identifies the patterns of change, if not always the magnitudes, indicating its usefulness as either a stand-alone tool or in combination with remote sensing data, for example, through the implementation of the "triangle" inversion modelling approach. On this basis, validation efforts presented herein are particularly important for all applications related to data assimilation, where ensuring that all model outputs are in close coherence to the physical processes being modelled are imperative to the successful development of such applications.

7 Concluding remarks

This study evaluated the ability of the SimSphere land biosphere model in predicting a number of parameters characterising land surface interactions for eight sites from the global terrestrial monitoring network, FLUXNET. A rigorous comparison was performed for 72 selected days in the year 2011. The main findings of this study are concluded as follows:

In overall, SimSphere estimates of instantaneous energy fluxes and air temperature showed good agreement in all ecosystems evaluated, apart from a minor underestimation of R_g and R_{net} (MBE = −19.48 and −16.49 W m^{-2} respectively). Some ecosystems exhibited poorer simulation accuracies than others, most noticeably cropland (US_IB1) and grazing pasture (Calperum); whilst the woodland savannah (Howard Springs) and mulga woodland (Alice Springs) ecosystems both attained the highest overall simulation accuracies. Comparisons showed a good agreement between modelled and measured fluxes, especially for the days with smoothed daily flux trends. Very high values of the Nash–Sutcliffe efficiency index were also reported for all parameters ranging from 0.720 to 0.998, suggesting a very good model representation of the observations. Highest simulation accuracies were obtained for the open woodland savannah and mulga woodland sites for most of the compared parameters.

The process of validating any physical model is imperative to understand its representation of real world scenarios. It helps to identify any deficiencies in the models' predictive ability and helps identify any possible sources of error and uncertainty associated with a model. To our knowledge, very few studies, if any, have acted to specifically validate SimSphere to numerous ecosystems in the USA and Australia. On this basis, with the currently expanding use of the model as either a stand-alone research or educational tool, or for its synergy with EO data, its validation is not only timely, but essential. SimSphere, despite its inherent architectural limitations can be applied in the future for solving various theoretical and applied tasks. The model presents itself as an important tool to acquire regional specific data, essential for numerous hydrological modelling, agriculture and water resource management applications. There is certainly room for further improvements to the model, in particular for developing it further in terms of its representation of the various physical processes characterising land surface interactions. This is a promising research direction on which future efforts should be focused. The development of this model could further its use as a helpful tool for educators, students, policy decision makers and researchers of environmental sciences alike.

Acknowledgements. This research was conducted with the support of the European Commission under the Marie Curie Re-Integration Grant "TRANSFORM-EO" project. Authors gratefully acknowledge the funding body for their financial support. Authors would also like to extend thank you to the PI's from the AmeriFlux and OzFlux networks for the data provision which made this study possible.

References

Akkermans, T., Thiery, W., and Van Lipzig, N. P.: The regional climate impact of a realistic future deforestation scenario in the Congo Basin, J. Climate, 27, 2714–2734, 2014.

Alexandris, S. and Kerkides., P.: New empirical formula for hourly estimations of reference evapotranspiration, Agr. Water Manage., 60, 157–180, 2003.

Aubinet, M., Grelle, A., Ibrom, A., Rannik, Ü., Moncrieff, J., Foken, T., Kowalski, A. S., Martin, P. H., Berbigier, P., Bernhofer, Ch., Clement, R., Elbers, J., Granier, A., Grünwald, T., Morgenstern, K., Pilegaard, K., Rebmann, C., Snijders, W., Valentini, R., and Vesala, T.: Estimates of the annual net carbon and water exchange of forests: the EUROFLUX methodology, Adv. Ecol. Res., 30, 113–175, 2000.

Barr, A. G., Morgenstern, K., Black, T. A., McCaughey, J. H., and Nesic, Z.: Surface energy balance closure by the eddy covariance method above three boreal forest stands and implications for the measurement of the CO_2 flux, Agr. Forest Meteorol., 140, 322–337, 2006.

Battrick, B. and Herland, E. A.: The Changing Earth. New Scientific Challenges for ESA's Living Planet Programme, ESA SP-1304, ESA, Publications Division, ESTC, the Netherlands, 2006.

Bellocchi, G., Rivington, M., Donatelli, M., and Matthews, K.: Validation of biophysical models: issues and methodologies, a review, Agron. Sustain. Dev., 30, 109–130, 2010.

Budyko, M. I.: The heat balance of the Earth's surface, Sov. Geogr., 2, 3–13, 1961.

Calperum Mallee SuperSite, Terrestrial Ecosystem Research Network: available at: http://www.tern-supersites.net.au/index.php/calperum, last access: 26 November 2014.

Carlson, T. N.: An overview of the "triangle method" for estimating surface evapotranspiration and soil moisture from satellite imagery, Sensors, 7, 1612–1629, 2007.

Carlson, T. N. and Boland, F. E.: Analysis of urban-rural canopy using a surface heat flux/temperature model, J. Appl. Meteorol., 17, 998–1013, 1978.

Carlson, T. N. and Lynn, B.: The effects of plant water storage on transpiration and radiometric surface temperature, Agr. Forest Meteorol., 57, 171–186, 1991.

Carlson, T. N., Dodd, J. K., Benjamin, S. G., and Cooper, J. N.: Satellite estimation of the surface energy balance, moisture availability and thermal inertia, J. Appl. Meteorol., 20, 6–87, 1981.

Castellvi, F., Martinez-Cob, A., and Perez-Coveta, O.: Estimating sensible and latent heat fluxes over rice using surface renewal, Agr. Forest Meteorol., 139, 164–169, 2006.

Chauhan, N. S., Miller, S., and Ardanuy, P.: Spaceborne soil moisture estimation at high resolution: a microwave-optical/IR synergistic approach, Int. J. Remote Sens., 22, 4599–4646, 2003.

Clapp, R. B. and Hornberger, G. M.: Empirical equations for some soil hydraulic-properties, Water Resour. Res., 14, 601–604, 1978.

Cosby, B. J., Hornberger, G. M., Clapp, R. B., and Ginn, T.: A statistical exploration of the relationships of soil moisture characteristics to the physical properties of soils, Water Resour. Res., 20, 682–690, 1984.

Coudert, B., Ottlé, C., and Briottet, X.: Monitoring land surface processes with thermal infrared data: calibration of SVAT parameters based on the optimisation of diurnal surface temperature cycling features, Remote Sens. Environ., 112, 872–887, 2008.

Cui, X. and Graf, H. F.: Recent land cover changes on the Tibetan Plateau: a review, Climatic Change, 94, 47–61, 2009.

Culf, A. D., Folken, T., and Gash., J. H. C.: The energy balance closure problem, in: Vegetation, Water, Humans and the Climate, Springer-Verlag, Berlin, 159–166, 2002.

Deardorff, J. W.: Efficient prediction of ground surface temperature and moisture, with inclusion of a layer of vegetation, J. Geophys. Res.-Oceans, 83, 1889–1903, 1978.

Dickinson, R. E. and Henderson-Sellers, A.: Modelling tropical deforestation: a study of GCM land-surface parametrizations, Q. J. Roy. Meteor. Soc., 114, 439–462, 1988.

European Space Agency: Support to Science Element, a Pathfinder for Innovation in Earth Observation, ESA, available at: http://due.esrin.esa.int/stse/files/document/STSE_report_121016.pdf (last access: 10 July 2014), 2012.

Fermi Agricultural Full Site Info, AmeriFlux, available at: http://ameriflux.ornl.gov/fullsiteinfo.php?sid=46, last access: 26 November 2014.

Fermi National Accelerator Laboratory – (Agricultural site), FLUXNET, available at: http://fluxnet.ornl.gov/site/899, last access: 26 November 2014.

Gillies, R. R.: Aphysically-Based Land Use Classification Scheme Using Remote Solar and Thermal Infrared Measurements Suitable for Describing Urbanisation, PhD Thesis, University of Newcastle, UK, 121 pp., 1993.

Gillies, R. R., Kustas, W. P., and Humes, K. S.: A verification of the "triangle" method for obtaining surface soil water content and energy fluxes from remote measurements of the Normalized Difference Vegetation Index (NDVI) and surface e, Int. J. Remote Sens., 18, 3145–3166, 1997.

GMDD

8, 2437–2495, 2015

Validating a 1-D SVAT model

G. P. Petropoulos et al.

Granz, D., Zhang, X., and Carlson., T. N.: Observations and model simulations link stomatal inhabitation to impaired hydraulic conductance following ozone exposure in cotton, Plant Cell Environ., 22, 1201–1210, 1999.
Hamilton, M. A.: Model validation: an annotated bibliography, Commun. Stat. Theory., 20, 2207–2266, 1991.
Hsu, M. H., Kuo, A. Y., Kuo, J. T., and Liu, W. C.: Procedure to calibrate and verify numerical models of estuarine hydrodynamics, J. Hydraul. Eng.-ASCE, 125, 166–182, 1999.
Huth, N. and Holzworth, D.: Common sense in model testing, in: Proc. MODSIM 2005 International Congress on Modelling and Simulation: Advances and Applications for Management and Decision Making, Melbourne, Australia, 12–15 December, edited by: Zerger, A. and Argent, R. M., 2804–2809, 2005.
Kramer, K., Leinonen, I., Bartelink, H., Berbigier, P., Borgnetti, M., Bernhofer, C., Cienciala, E., Dolman, A. J., Froer, O., Gracia, A., Granier, A., Grunwald, T., Hari, P., Jans, W., Kellomaki, S., Loustau, D., Magnani, F., Markkanen, T., Matteucci, G., Mohren, G. M., Moors, E., Nissenen, A., Peltola, H., Sabate, S., Sanchez, A., Sontag, M., Valentini, R., and, Vesala., T.: Evaluation of six-process-based forest growth models using eddy-covariance measurements of CO_2 and H_2O fluxes at six forest sites in Europe, Glob. Change Biol., 8, 213–230, 2002.
Koirala, S., Yeh, P. J. F., Hirabayashi, Y., Kanae, S., and Oki, T.: Global-scale land surface hydrologic modelling with the representation of water table dynamics, J. Geophys. Res.-Atmos., 119, 75–89, 2014.
Liu, Y., Hiyama, T., and Yamaguchi, Y.: Scaling of land surface temperature using satellite data: a case examination on ASTER and MODIS products over a heterogeneous terrain area, Remote. Sens. Environ., 105, 115–128, 2006.
Lucky Hills Shrubland Full Site Info, AmeriFlux, available at: http://ameriflux.ornl.gov/fullsiteinfo.php?sid=216, last access: 26 November 2014.
Lynn, B. H. and Carlson, T. N.: A stomatal resistance model illustrating plant vs. external control of transpiration, Agr. Forest Meteorol., 52, 5–43, 1990.
Maayar, M., Price, D. T., Delire, C., Foley, J. A., Black, T. A., and Bessemoulin, P.: Validation of the integrated biosphere simulator over Canadian deciduous and coniferous boreal forest stands, J. Geophys. Res.-Atmos., 106, 14339–14355, 2001.
Manabe, S.: Climate and the ocean circulation 1: I. The atmospheric circulation and the hydrology of the Earth's surface, Mon. Weather Rev., 97, 739–774, 1969.

GMDD
8, 2437–2495, 2015

Marshall, M., Tu, K., Funk, C., Michaelsen, J., Williams, P., Williams, C., Ardö, J., Boucher, M., Cappelaere, B., de Grandcourt, A., Nickless, A., Nouvellon, Y., Scholes, R., and Kutsch, W.: Improving operational land surface model canopy evapotranspiration in Africa using a direct remote sensing approach, Hydrol. Earth Syst. Sci., 17, 1079–1091, doi:10.5194/hess-17-1079-2013, 2013.

Mascart, P., Taconet, O., Pinty, J. P., and Mehrez, M. B.: Canopy resistance formulation and its effect in mesoscale models: a HAPEX perspective, Agr. Forest Meteorol., 54, 319–351, 1991.

Missouri Ozark Full Site Info, AmeriFlux, available at: http://ameriflux.ornl.gov/fullsiteinfo.php?sid=64, last access: 26 November 2014.

Monin, A. S. and Obukhov, A.: Basic laws of turbulent mixing in the surface layer of the atmosphere, Contrib. Geophys. Inst. Acad. Sci. USSR, 151, 163–187, 1954.

Monitoring Sites – Alice Springs, OzFlux, available at: http://www.ozflux.org.au/monitoringsites/alicesprings/index.html#intro, last access: 26 November 2014.

Monitoring Sites – Calperum, OzFlux, available at: http://www.ozflux.org.au/monitoringsites/calperum/calperum_description.html, last access: 26 November 2014.

Monitoring Sites – Howard Springs, OzFlux, available at: http://www.ozflux.org.au/monitoringsites/howardsprings/howardsprings_description.html, last access: 26 November 2014.

Nash, J. and Sutcliffe, J. V.: River flow forecasting through conceptual models, Part I – A discussion of principles, J. Hydrol., 10, 282–290, 1970.

Olchev, A., Ibrom, A., Ross, T., Falk, U., Rakkibu, G., Radler, K., Grotea, S., Kreileina, H., and Gravenhorst, G.: A modelling approach for simulation of water and carbon dioxide exchange between multi-species tropical rain forest and the atmosphere, Ecol. Modell., 212, 122–130, 2008.

Olioso, A., Carlson, T. N., and Brisson., N.: Simulation of diurnal transpiration and photosynthesis of a water stressed soybean crop, Agr. Forest Meteorol., 81, 41–59, 1996.

Olioso, A., Braud, I., Chanzy, A., Courault, D., Demarty, J., Kergoat, L., and Wigneron, J. P.: SVAT modeling over the Alpilles-ReSeDA experiment: comparing SVAT models over wheat fields, Agronomie-Sciences des Productions Vegetales et de l'Environnement, 22, 651–668, 2002.

Papale, D., Reichstein, M., Aubinet, M., Canfora, E., Bernhofer, C., Kutsch, W., Longdoz, B., Rambal, S., Valentini, R., Vesala, T., and Yakir, D.: Towards a standardized processing of Net

Ecosystem Exchange measured with eddy covariance technique: algorithms and uncertainty estimation, Biogeosciences, 3, 571–583, doi:10.5194/bg-3-571-2006, 2006.
Pedinotti, V.: The SWOT Satellite Mission: Contribution of the Large Swath Altimetry for Improving the Hydrological and Hydrodynamic Processes of a Large Scale Model, PhD thesis, Institut National Polytechnique de Toulouse, France, 2013.
Petropoulos, G. and Carlson, T. N.: Retrievals of turbulent heat fluxes and soil moisture content by remote sensing, in: Advances in Environmental Remote Sensing: Sensors, Algorithms, and Applications, Taylor and Francis, Boca Raton, FL, USA, 556, 667–502, 2011.
Petropoulos, G., Carlson, T., and Wooster, M. J.: An overview of the use of the SimSphere Soil Vegetation Atmospheric Transfer (SVAT) model for the study of land atmosphere interactions, Sensors, 9, 4286–4308, 2009a.
Petropoulos, G., Wooster, M. J., Kennedy, K., Carlson, T. N., and Scholze, M.: A global sensitivity analysis study of the 1d SimSphere SVAT model using the GEM SA software, Ecol. Model., 220, 2427–2440, 2009b.
Petropoulos, G. P., Griffiths, H. M., and Tarantola, S.: Towards operational products development from Earth observation: exploration of SimSphere land surface process model sensitivity using a GSA approach, in: 7th International Conference on Sensitivity Analysis of 25 Model Output, Nice, France, 1–4 July 2013, 2013a.
Petropoulos, G., Griffiths, H. M., and Ioannou-Katidis, P.: Sensitivity exploration of SimSphere land surface model towards its use for operational products development from Earth observation data, Chapter 14, in: Advancement in Remote Sensing for Environmental Applications, edited by: Mukherjee, S., Gupta, M., Srivastava, P. K., and Islam, T., Springer International Publishing, Cham, Switzerland, 35–56, 2013b.
Petropoulos, G. P., Griffiths, H., and Tarantola, S.: Sensitivity analysis of the SimSphere SVAT model in the context of EO-based operational products development, Environ. Modell. Softw., 49, 166–179, 2013c.
Petropoulos, G. P., Konstas, I., and Carlson, T. N.: Automation of SimSphere Land Surface Model Use as a standalone application and integration with EO data for deriving key land surface parameters, in: European Geosciences Union, Vienna, Austria, 7–12 April 2013, p. 14162, 2013d.
Petropoulos, G. P., Griffiths, H., Dorigo, W., Xaver, A., and Gruber, A.: Surface soil moisture estimation: significance, controls and conventional measurement techniques, in: Remote Sens-

GMDD
8, 2437–2495, 2015

Validating a 1-D SVAT model

G. P. Petropoulos et al.

ing of Energy Fluxes and Soil Moisture Content, edited by: Petropoulos, G. P., Taylor and Francis, ISBN: 978-1-4665-0578, 29–48, 2013e.
Petropoulos, G. P., Griffiths, H. M., Carlson, T. N., Ioannou-Katidis, P., and Holt, T.: SimSphere model sensitivity analysis towards establishing its use for deriving key parameters characterising land surface interactions, Geosci. Model Dev., 7, 1873–1887, doi:10.5194/gmd-7-1873-2014, 2014.
Piles, M., Camps, A., Vall-Llossera, M., Corbella, I., Panciera, R., Rudiger, C., Kerr, Y. H., and Walker, J.: Downscaling SMOS-derived soil moisture using MODIS visible/infrared data, IEEE T. Geosci. Remote Se., 49, 3156–3166, 2011.
Prentice, I. C., Liang, X., Medlyn, B. E., and Wang, Y.-P.: Reliable, robust and realistic: the three R's of next-generation land surface modelling, Atmos. Chem. Phys. Discuss., 14, 24811–24861, doi:10.5194/acpd-14-24811-2014, 2014.
Ridler, M. E., Sandholt, I., Butts, M., Lerer, S., Mougin, E., Timouk, F., Kergoat, L., and Madsen, H.: Calibrating a soil–vegetation–atmosphere transfer model with remote sensing estimates of surface temperature and soil surface moisture in a semi-arid environment, J. Hydrol., 436, 1–12, 2012.
Rosolem, R., Gupta, H. V., Shuttleworth, W. J., Gonçalves, L. G. G., and Zeng, X.: Towards a comprehensive approach to parameter estimation in land surface parameterization schemes, Hydrol. Process., 27, 2075–2097, 2013.
Ross, S. L. and Oke, T. R.: Tests of three urban energy balance models, Bound.-Lay. Meteorol., 44, 73–96, 1988.
Second Space for Hydrology Workshop, European Space Agency (ESA): available at: http://earth.esa.int/hydrospace07/, last access: 16 December 2014.
Sellers, P. J., Mintz, Y. C. S. Y., Sud, Y. E. A., and Dalcher, A.: A simple biosphere model (SiB) for use within general circulation models, J. Atmos. Sci., 43, 505–531, 1986.
Sellers, P. J., Dickinson, R. E., Randall, D. A., Betts, A. K., Hall, F. G., Berry, J. A., Collatz, G. J., Denning, A. S., Mooney, H. A., Nobre, C. A., Sato, N., Field, C. B., and Henderson-Sellers, A.: Modelling the exchanges of energy, water, and carbon between continents and the atmosphere, Science, 275, 502–509, 1997.
Sheikh, V., Visser, S., and Stroosnijder, L.: A simple model to predict soil moisture: Bridging Event and Continuous Hydrological (BEACH) modelling, Environ. Modell. Softw., 24, 542–556, 2009.

Stoyanova, J. S. and Georgiev, C. G.: SVAT modelling in support to flood risk assessment in Bulgaria, Atmos. Res., 123, 384–399, 2013.
Taconet, O., Carlson, T., Bernard, R., and Vidal-Madjar, D.: Evaluation of a surface/vegetation parameterisation using satellite measurements of surface temperature, J. Clim. Appl. Meteorol., 25, 1752–1767, 1986.
Todhunter, P. E. and Terjung, W. H.: Intercomparison of three urban climate models, Bound.-Lay. Meteorol., 42, 181–205, 1987.
Tonzi Ranch Full Site Info, AmeriFlux, available at: http://ameriflux.ornl.gov/fullsiteinfo.php?sid=29, last access: 26 November 2014.
Twine, T. E., Kustas, W. P., Norman, J. M., Cook, D. R., Houser, P., Meyers, T. P., Prueger, J. H., Tarks, P. J., and Wesley, M. L.: Correcting eddy-covariance flux underestimates over a grassland, Agr. Forest Meteorol., 103, 279–300, 2000.
Vaira Ranch Full Site Info, AmeriFlux, available at: http://ameriflux.ornl.gov/fullsiteinfo.php?sid=30, last access: 26 November 2014.
Verbeeck, H., Samson, R., Granier, A., Montpied, P., and Lemeur, R.: Multi-year model analysis of GPP in a temperate beech forest in France, Ecol. Model., 210, 85–109, 2008.
Wallach, D.: Evaluating crop models, in: Working with Dynamic Crop Models, edited by: Wallach, D., Makowski, D., and Jones, J. W., Elsevier, Amsterdam, the Netherlands, 11–53, 2006.
Walnut Gulch Experimental Watershed, USDA, available at: http://ars.usda.gov/PandP/docs.htm?docid=10978&page=2, last access: 26 November 2014.
Wilson, K. B. and Baldocchi, D. D.: Seasonal and inter-annual variability of energy fluxes over a broadleaved temperate deciduous forest in North America, Agr. Forest Meteorol., 100, 1–18, 2000.
Wilson, K., Carlson, T., and Bunce, J. A.: Feedback significantly influences the simulated effect of CO_2 on seasonal evapotranspiration from two agricultural species, Glob. Change Biol., 5, 903–917, 1999.
Wilson, K., Goldstein, A., Falge, E., Aubinet, M., Baldocchi, D., Berbigier, P., and Verma, S.: Energy balance closure at FLUXNET sites, Agr. Forest Meteorol., 113, 223–243, 2002.

Table 1. Summary of the main SimSphere inputs. The units of each of the model inputs are also provided in parentheses where applicable.

Name of the model input	Process in which parameter is involved	Min value	Max value
Slope (degrees)	TIME and LOCATION	0	45
Aspect (degrees)	TIME and LOCATION	0	360
Station Height (meters)	TIME and LOCATION	0	4.92
Fractional Vegetation Cover (%)	VEGETATION	0	100
LAI ($m^2 m^{-2}$)	VEGETATION	0	10
Foliage emissivity (unitless)	VEGETATION	0.951	0.990
[Ca] (external [CO_2] in the leaf) (ppmv)	VEGETATION	250	710
[Ci] (internal [CO_2] in the leaf) (ppmv)	VEGETATION	110	400
[O3] (ozone concentration in the air) (ppmv)	VEGETATION	0.0	0.25
Vegetation height (meters)	VEGETATION	0.021	20.0
Leaf width (meters)	VEGETATION	0.012	1.0
Minimum Stomatal Resistance ($s m^{-1}$)	PLANT	10	500
Cuticle Resistance ($s m^{-1}$)	PLANT	200	2000
Critical leaf water potential (bar)	PLANT	−30	−5
Critical solar parameter ($W m^{-2}$)	PLANT	25	300
Stem resistance ($s m^{-1}$)	PLANT	0.011	0.150
Surface Moisture Availability ($vol\,vol^{-1}$)	HYDROLOGICAL	0	1
Root Zone Moisture Availability ($vol\,vol^{-1}$)	HYDROLOGICAL	0	1
Substrate Max. Volum. Water Content ($vol\,vol^{-1}$)	HYDROLOGICAL	0.01	1
Substrate climatol. mean temperature (°C)	SURFACE	20	30
Thermal inertia ($W m^{-2} K^{-1}$)	SURFACE	3.5	30
Ground emissivity (unitless)	SURFACE	0.951	0.980
Atmospheric Precipitable water (cm)	METEOROLOGICAL	0.05	5
Surface roughness (meters)	METEOROLOGICAL	0.02	2.0
Obstacle height (meters)	METEOROLOGICAL	0.02	2.0
Fractional Cloud Cover (%)	METEOROLOGICAL	1	10
RKS (satur. thermal conduct.) (Cosby et al., 1984)	SOIL	0	10
Cosby B (see Cosby et al., 1984)	SOIL	2.	12.
THM (satur. vol. water cont.) (Cosby et al., 1984)	SOIL	0.3	0.5
PSI (satur. water potential) (Cosby et al., 1984)	SOIL	1	7
Wind direction (degrees)	WIND SOUNDING PROFILE		360
Wind speed (knots)	WIND SOUNDING PROFILE	–	–
Altitude (1000's feet)	WIND SOUNDING PROFILE	–	–
Pressure (mBar)	MOISTURE SOUNDING PROFILE	–	–
Temperature (Celsius)	MOISTURE SOUNDING PROFILE	–	–
Temperature – Dewpoint Temperature (Celsius)	MOISTURE SOUNDING PROFILE	–	–

GMDD
8, 2437–2495, 2015

Table 2. Site descriptions of chosen sites.

Site Name	Site Abbreviation	Country	Geographic Location	PFT	Ecosystem Type	Dominant Species	Elevation	Climate
Alice Springs	–	Australia	−22.283/133.249	MWO	Mulga Woodland	*Acacia aneura*	606 m	Desert: hot and dry summers and cold winters
Calperum	–	Australia	−34.003/140.588	PAS	Grazing Pasture	*Eucalyptus stricta*	200 m	Subtropical dry summer
Howard Springs	–	Australia	−12.495/131.15	WSV	Woody Savannah	*Eucalyptus miniata* and *Eucalyptus tentrodonata*	64 m	Tropical wet and dry: hot and humid summers
Vaira Ranch	US_VAR	USA	38.406/−120.950	GRA	Grassland	*Brachypodium distachyon*, *Hypochaeris glabr*, *Trifolium dubium*	129 m	Mediterranean: hot and dry summers, wet and cold winters
Missouri Ozark	US_MOZ	USA	38.7441/−92.200	DBL	Deciduous Broadleaf	*Quercus alba*, *Quercus velutina*, *Carya ovata*	219 m	Temperate continental
Fermi Agricultural	US_IB1	USA	41.8593/−88.2227	CRO	Cropland	Soybean (C3)	225 m	Wet and hot summers and mild winters
Tonzi Ranch	US_TON	USA	38.4316/−120.9660	WSV	Woody Savannah	*Quercus douglasii*, *Pinus sabiniana*, *Brachypodium distachyon*	169 m	Mediterranean: hot and dry summers, wet and cold winters
Lucky Hills Shrubland	US_WHS	USA	31.7438/−110.0522	SHR	Shrubland	*Larrea tridentate*, *Acacia constricta*, *Flourensia cernua*	1372 m	Semi-Arid

GMDD
8, 2437–2495, 2015

Table 3. Daily simulation accuracy and average site simulation accuracy for R_g fluxes. Bias, scatter, RMSD and MAE are expressed in $W m^{-2}$. NASH index is unitless.

		Statistical Test				
Location	Date	Bias	Scatter	RMSD	MAE	NASH
Alice Springs	23 Mar 2011	−5.530	33.379	33.834	24.735	0.998
	15 Apr 2011	13.560	28.838	31.867	19.104	0.956
	23 Apr 2011	3.956	29.619	29.882	19.365	0.974
	10 May 2011	1.817	20.403	20.483	13.407	0.979
	24 May 2011	−16.473	25.452	30.318	20.285	0.924
	31 May 2011	−13.523	21.885	25.726	17.083	0.996
	18 Jun 2011	−26.928	32.748	42.397	28.033	0.949
	25 Jun 2011	−35.779	39.466	53.270	35.838	0.993
	18 Jul 2011	−34.001	33.934	48.038	34.001	1.000
	20 Aug 2011	−48.375	40.444	63.055	48.375	0.975
	Average	−19.480	62.362	67.825	46.286	0.974
Calperum	24 Feb 2011	9.675	23.062	25.009	19.077	0.994
	2 Mar 2011	8.408	22.628	24.139	18.314	0.979
	31 Mar 2011	30.482	28.252	41.561	30.482	0.986
	24 Apr 2011	41.932	33.666	53.775	41.932	0.975
	22 Jul 2011	−58.276	61.061	84.407	60.624	0.978
	28 Jul 2011	−67.865	71.010	98.224	70.950	0.974
	28 Aug 2011	−108.134	102.924	149.286	110.484	0.889
	1 Dec 2011	−110.334	75.487	133.685	112.586	0.899
	23 Dec 2011	−76.000	62.661	98.501	78.332	0.978
	29 Dec 2011	−74.103	62.080	96.670	76.348	0.991
	Average	−40.421	80.911	90.446	61.913	0.964
Howard Springs	18 Apr 2011	18.241	20.763	27.637	18.784	0.975
	23 Apr 2011	7.810	15.149	17.044	11.637	0.978
	13 May 2011	−0.928	20.238	20.259	15.108	0.989
	27 May 2011	24.470	29.618	38.419	25.104	0.978
	3 Jun 2011	−8.373	34.642	35.640	27.598	0.935
	14 Jun 2011	−20.948	43.618	48.387	35.502	0.974
	22 Jun 2011	−15.483	42.380	45.120	33.863	0.976
	22 Jul 2011	−37.300	56.845	67.990	48.955	0.982
	28 Jul 2011	−63.827	69.493	94.356	67.300	0.989
	27 Sep 2011	−52.796	51.872	74.014	54.038	0.979
	Average	−14.913	50.367	52.528	33.789	0.976
US_MOZ	28 Jun 2011	−48.127	51.404	70.417	59.862	0.976
	1 Aug 2011	−5.549	34.912	35.350	24.808	0.976
	18 Aug 2011	−2.574	35.531	35.625	27.927	0.991
	31 Aug 2011	42.462	42.043	59.755	42.462	0.974
	1 Sep 2011	34.475	30.616	46.107	34.475	0.978
	7 Sep 2011	4.829	41.094	41.377	30.595	0.987
	12 Sep 2011	16.178	33.508	37.209	24.666	0.969
	30 Sep 2011	29.144	34.415	45.098	29.218	0.988
	29 Sep 2011	42.099	34.044	54.142	42.099	0.978
	11 Nov 2011	48.522	44.135	65.592	48.522	0.972
	Average	16.496	47.582	50.360	36.570	0.979

GMDD
8, 2437–2495, 2015

Table 3. Continued.

Location	Date	Statistical Test Bias	Scatter	RMSD	MAE	NASH
US_IB1	30 May 2011	−70.936	67.440	97.878	70.936	0.939
	7 Jun 2011	−64.456	68.097	93.764	65.039	0.898
	28 Jun 2011	−69.642	69.189	98.169	72.247	0.899
	8 Jul 2011	−55.803	74.499	93.081	67.981	0.937
	24 Aug 2011	7.956	56.423	56.982	38.417	0.986
	13 Sep 2011	12.639	43.928	45.710	31.172	0.978
	15 Sep 2011	−2.542	43.422	43.496	29.897	0.940
	1 Oct 2011	13.797	42.181	44.380	27.308	0.977
	15 Oct 2011	12.389	47.002	48.607	29.417	0.949
	24 Oct 2011	15.150	45.931	48.365	28.506	0.997
	Average	−20.145	68.202	71.114	46.092	0.950
US_TON	27 Feb 2011	39.369	24.889	46.577	39.682	0.961
	17 Mar 2011	−88.374	74.907	115.849	88.374	0.899
	24 May 2011	−77.275	51.048	92.614	77.275	0.961
	24 Jun 2011	−62.150	40.586	74.228	62.150	0.965
	30 Jul 2011	−10.444	17.099	20.036	15.339	0.973
	7 Aug 2011	−19.860	27.433	33.867	24.868	0.984
	28 Aug 2011	−1.790	19.710	19.791	14.832	0.991
	15 Sep 2011	46.816	36.149	59.148	46.816	0.974
	1 Nov 2011	66.774	55.125	86.588	66.774	0.925
	16 Nov 2011	58.468	50.651	77.356	58.468	0.941
	Average	−4.846	69.543	69.712	49.458	0.957
US_WHS	8 Feb 2011	−119.413	122.286	170.919	119.474	0.899
	16 Feb 2011	−124.624	114.719	169.386	124.624	0.845
	25 Mar 2011	−141.666	114.856	182.376	141.666	0.880
	22 Jun 2011	−73.152	48.543	87.793	73.152	0.937
	13 Jul 2011	−77.116	63.048	99.609	78.604	0.913
	2 Aug 2011	−42.919	63.541	76.677	59.743	0.986
	28 Aug 2011	−21.540	47.973	52.587	41.999	0.983
	3 Aug 2011	−11.917	36.705	38.591	29.599	0.997
	5 Oct 2011	−1.315	35.017	35.041	24.874	0.985
	20 Oct 2011	11.969	27.147	29.669	18.541	0.991
	Average	−56.400	83.364	100.651	67.452	0.942
All Sites Average		−19.480	62.362	67.825	46.424	0.963

GMDD
8, 2437–2495, 2015

Table 4. Daily simulation accuracy and average site simulation accuracy for R_{net} fluxes. Bias, scatter, RMSD and MAE are expressed in $W\,m^{-2}$. NASH index is unitless.

		Statistical Test				
Location	Date	Bias	Scatter	RMSD	MAE	NASH Index
Alice Springs	23 Mar 2011	−47.837	39.660	62.140	49.882	0.989
	15 Apr 2011	5.372	20.583	21.273	15.351	0.978
	23 Apr 2011	5.824	20.028	20.858	15.026	0.982
	10 May 2011	0.238	19.916	19.917	16.857	0.981
	24 May 2011	15.020	14.517	20.889	17.071	0.968
	31 May 2011	−16.367	18.303	24.554	20.454	0.991
	18 Jun 2011	−32.891	21.068	39.061	34.370	0.974
	25 Jun 2011	−40.447	18.120	44.321	40.619	0.979
	18 Jul 2011	−17.876	11.168	21.078	18.283	0.998
	20 Aug 2011	−34.572	13.290	37.038	34.572	0.964
	Average	−16.354	29.693	33.898	26.248	0.980
Calperum	24 Feb 2011	28.310	33.371	43.762	38.932	0.979
	2 Mar 2011	2.225	22.545	22.655	17.920	0.998
	31 Mar 2011	10.283	26.718	28.628	24.488	0.982
	24 Apr 2011	36.988	44.560	57.911	49.755	0.981
	22 Jul 2011	−62.631	39.682	74.143	62.631	0.968
	28 Jul 2011	−42.477	38.926	57.615	42.561	0.964
	28 Aug 2011	−76.722	58.516	96.490	76.722	0.945
	1 Dec 2011	−70.835	52.791	88.343	74.163	0.911
	23 Dec 2011	−18.274	33.556	38.209	26.074	0.965
	29 Dec 2011	−40.989	41.011	57.982	42.622	0.971
	Average	−23.412	56.457	61.119	45.587	0.966
Howard Springs	18 Apr 2011	22.799	32.616	39.794	32.824	0.963
	23 Apr 2011	17.030	30.418	34.861	28.659	0.944
	13 May 2011	40.734	28.011	49.435	40.770	0.956
	27 May 2011	54.627	44.721	70.598	56.139	0.939
	3 Jun 2011	20.033	27.166	33.753	25.206	0.985
	14 Jun 2011	16.257	33.676	37.394	29.818	0.985
	22 Jun 2011	10.769	39.441	40.885	29.577	0.989
	22 Jul 2011	−0.606	34.490	34.496	26.795	0.967
	28 Jul 2011	−51.747	47.364	70.151	57.362	0.995
	27 Sep 2011	−26.446	29.775	39.824	30.196	0.997
	Average	10.345	45.894	47.046	35.735	0.972
US_VAR	10 May 2011	−32.459	19.863	38.054	32.459	0.974
	23 Jun 2011	−36.762	33.668	49.850	44.402	0.987
	19 Jul 2011	−10.809	34.629	36.277	31.926	0.989
	30 Jul 2011	−2.925	49.866	49.952	43.812	0.974
	7 Aug 2011	4.385	40.179	40.418	32.472	0.911
	27 Aug 2011	40.924	61.807	74.128	68.505	0.978
	22 Sep 2011	43.978	65.161	78.613	72.562	0.946
	7 Oct 2011	−2.192	85.263	85.291	78.183	0.998
	26 Nov 2011	3.421	61.113	61.209	54.674	0.996
	19 Dec 2011	−8.416	47.347	48.089	43.567	0.996
	Average	−0.086	58.640	58.640	50.256	0.975

GMDD
8, 2437–2495, 2015

Table 4. Continued.

Location	Date	Bias	Scatter	RMSD	MAE	NASH Index
		Statistical Test				
US_MOZ	28 Jun 2011	−88.456	58.743	106.185	91.190	0.957
	1 Aug 2011	−8.963	31.829	33.067	23.318	0.984
	18 Aug 2011	−29.156	31.881	43.203	38.600	0.989
	31 Aug 2011	−7.511	36.159	36.931	31.741	0.969
	1 Sep 2011	5.452	26.086	26.649	20.742	0.968
	7 Sep 2011	−26.395	51.749	58.092	43.978	0.964
	12 Sep 2011	−2.297	29.744	29.833	23.891	0.981
	30 Sep 2011	−17.849	46.086	49.421	37.056	0.991
	29 Sep 2011	33.277	35.388	48.576	33.769	0.905
	11 Nov 2011	54.811	64.019	84.278	56.086	0.886
	Average	−13.251	49.828	51.560	38.463	0.959
US_IB1	30 May 2011	−86.392	70.851	111.729	86.392	0.842
	7 Jun 2011	−35.433	40.050	53.474	37.861	0.986
	28 Jun 2011	−38.581	33.741	51.253	40.592	0.972
	8 Jul 2011	−52.017	19.964	55.716	52.017	0.976
	24 Aug 2011	19.225	54.203	57.511	41.642	0.946
	13 Sep 2011	15.256	54.046	56.158	48.644	0.977
	15 Sep 2011	−1.686	70.254	70.274	59.803	0.899
	1 Oct 2011	15.906	58.936	61.045	45.117	0.985
	15 Oct 2011	24.753	73.015	77.097	68.475	0.978
	24 Oct 2011	−28.900	73.818	79.274	71.183	0.996
	Average	−16.787	67.536	69.591	55.173	0.956
US_TON	27 Feb 2011	−101.395	51.665	113.799	101.395	0.911
	17 Mar 2011	−88.306	35.392	95.134	88.306	0.913
	24 May 2011	−70.176	38.189	79.894	70.176	0.952
	24 Jun 2011	−83.358	42.987	93.789	83.358	0.962
	30 Jul 2011	−65.261	42.108	77.666	66.645	0.986
	7 Aug 2011	−53.888	54.313	76.511	58.276	0.965
	28 Aug 2011	−39.974	57.084	69.689	58.785	0.971
	15 Sep 2011	2.418	38.270	38.346	30.944	0.966
	1 Nov 2011	26.561	47.529	54.448	46.087	0.984
	16 Nov 2011	12.423	48.779	50.337	48.184	0.963
	Average	−46.096	62.963	78.033	65.216	0.957
US_WHS	8 Feb 2011	−56.655	73.692	92.953	66.574	0.912
	16 Feb 2011	−71.448	65.152	96.694	75.321	0.872
	25 Mar 2011	−70.666	57.327	90.995	75.110	0.874
	22 Jun 2011	−55.389	72.621	91.333	59.755	0.929
	13 Jul 2011	−10.839	27.379	29.446	23.781	0.985
	2 Aug 2011	−15.370	36.240	39.365	30.578	0.964
	28 Aug 2011	5.330	26.535	27.065	18.491	0.996
	3 Aug 2011	−24.342	51.801	57.235	41.300	0.996
	5 Oct 2011	48.880	27.232	55.954	48.880	0.968
	20 Oct 2011	8.068	52.600	53.215	50.053	0.978
	Average	−26.238	64.522	69.653	50.271	0.947
All Sites Average		−16.485	54.442	58.692	45.904	0.964

GMDD
8, 2437–2495, 2015

Validating a 1-D SVAT model

G. P. Petropoulos et al.

Table 5. Daily simulation accuracy and average site simulation accuracy for LE fluxes. Bias, scatter, RMSD and MAE are expressed in $\mathrm{W\,m^{-2}}$. NASH index is unitless.

Location	Date	Statistical Test Bias	Scatter	RMSD	MAE	NASH Index
Alice Springs	23 Mar 2011	−23.748	45.451	51.281	36.845	0.997
	15 Apr 2011	−17.304	23.039	28.813	19.958	0.992
	23 Apr 2011	2.759	23.883	24.042	14.129	0.989
	10 May 2011	20.870	19.876	28.820	21.319	0.935
	24 May 2011	4.588	4.682	6.556	5.443	0.969
	31 May 2011	5.122	8.633	10.038	6.646	0.968
	18 Jun 2011	−0.340	8.606	8.612	6.997	0.979
	25 Jun 2011	3.245	9.218	9.773	7.448	0.950
	18 Jul 2011	12.900	13.326	18.547	13.416	0.914
	20 Aug 2011	19.435	14.833	24.449	19.435	0.758
	Average	2.753	24.592	24.746	15.164	0.945
Calperum	24 Feb 2011	−9.768	31.404	32.888	23.057	0.995
	2 Mar 2011	−13.833	25.928	29.387	21.173	0.992
	31 Mar 2011	−8.476	18.346	20.210	13.190	0.994
	24 Apr 2011	−8.256	17.957	19.764	13.198	0.990
	22 Jul 2011	−7.970	15.525	17.452	10.971	0.979
	28 Jul 2011	−9.238	13.332	16.220	11.538	0.983
	28 Aug 2011	−17.687	24.638	30.329	19.448	0.979
	1 Dec 2011	−5.219	20.111	20.777	15.761	0.988
	23 Dec 2011	24.569	39.140	46.212	31.747	0.993
	29 Dec 2011	−11.570	30.292	32.426	24.782	0.993
	Average	−6.745	27.195	28.019	18.486	0.989
Howard Springs	18 Apr 2011	−31.861	46.214	56.132	40.757	0.997
	23 Apr 2011	−17.902	77.002	79.055	46.292	0.998
	13 May 2011	−5.362	23.187	23.799	17.167	0.997
	27 May 2011	35.698	44.908	57.368	39.407	0.970
	3 Jun 2011	26.117	37.604	45.784	29.793	0.976
	14 Jun 2011	7.114	16.137	17.636	12.012	0.984
	22 Jun 2011	31.513	35.670	47.597	36.329	0.982
	22 Jul 2011	13.300	29.131	32.023	20.232	0.993
	28 Jul 2011	−10.936	20.673	23.387	17.390	0.996
	27 Sep 2011	−25.350	70.484	74.904	39.027	0.965
	Average	2.233	50.064	50.114	29.841	0.986
US_VAR	10 May 2011	−9.006	13.063	15.867	12.657	0.968
	23 Jun 2011	29.672	38.127	48.313	31.897	0.978
	19 Jul 2011	23.914	29.524	37.994	25.480	0.928
	30 Jul 2011	27.988	31.607	42.218	29.019	0.292
	7 Aug 2011	22.118	25.558	33.800	22.975	0.654
	27 Aug 2011	24.328	29.460	38.207	24.560	0.665
	22 Sep 2011	17.852	21.536	27.973	17.852	0.414
	7 Oct 2011	6.588	27.196	27.983	19.533	0.979
	26 Nov 2011	−2.671	13.199	13.467	8.576	0.992
	19 Dec 2011	−2.613	10.597	10.914	7.207	0.985
	Average	13.817	28.932	32.062	19.976	0.786

Table 5. Continued.

Location	Date	Bias	Scatter	RMSD	MAE	NASH Index
			Statistical Test			
US_MOZ	28 Jun 2011	−11.798	56.091	57.318	43.455	0.912
	1 Aug 2011	66.840	84.613	107.828	73.193	0.912
	18 Aug 2011	25.063	59.741	64.785	45.616	0.937
	31 Aug 2011	37.947	49.678	62.513	41.236	0.912
	1 Sep 2011	46.763	62.264	77.869	53.781	0.927
	7 Sep 2011	21.021	48.810	53.144	38.273	0.869
	12 Sep 2011	40.564	50.338	64.648	45.217	0.945
	30 Sep 2011	15.956	38.187	41.386	28.549	0.974
	29 Sep 2011	16.384	35.632	39.218	35.565	0.945
	11 Nov 2011	28.345	32.973	43.482	32.720	0.841
	Average	25.653	55.918	61.522	42.019	0.917
US_IB1	30 May 2011	−28.883	61.843	68.255	54.172	0.899
	7 Jun 2011	40.289	71.267	81.867	65.317	0.927
	28 Jun 2011	32.156	51.861	61.020	49.594	0.982
	8 Jul 2011	−35.322	28.667	45.491	35.356	0.947
	24 Aug 2011	1.744	37.107	37.148	31.067	0.972
	13 Sep 2011	−1.044	50.497	50.508	43.883	0.821
	15 Sep 2011	−6.303	15.446	16.682	13.247	0.998
	1 Oct 2011	0.797	37.226	37.235	28.781	0.964
	15 Oct 2011	38.306	53.743	65.997	52.644	0.979
	24 Oct 2011	−14.133	17.310	22.347	18.556	0.978
	Average	2.761	52.468	52.540	39.262	0.947
US_TON	27 Feb 2011	−5.845	22.864	23.599	17.434	0.981
	17 Mar 2011	−16.497	43.055	46.107	32.990	0.969
	24 May 2011	−56.284	73.754	92.777	62.516	0.899
	24 Jun 2011	−3.138	35.440	35.579	27.232	0.948
	30 Jul 2011	6.049	29.060	29.683	20.932	0.969
	7 Aug 2011	2.088	20.960	21.064	16.994	0.990
	28 Aug 2011	0.902	16.514	16.539	11.705	0.985
	15 Sep 2011	7.753	22.493	23.791	14.024	0.983
	1 Nov 2011	−2.224	14.102	14.276	11.118	0.991
	16 Nov 2011	4.304	10.099	10.978	7.151	0.987
	Average	−6.289	38.274	38.788	22.210	0.970
US_WHS	8 Feb 2011	9.606	12.404	15.688	10.347	0.886
	16 Feb 2011	1.025	7.802	7.869	4.609	0.946
	25 Mar 2011	−0.038	5.984	5.984	4.216	0.925
	22 Jun 2011	−2.637	6.020	6.572	4.470	0.913
	13 Jul 2011	−5.690	21.219	21.968	16.753	0.956
	2 Aug 2011	−43.529	36.735	56.958	44.832	0.975
	28 Aug 2011	−39.800	37.571	54.732	41.242	0.979
	3 Aug 2011	−12.716	15.970	20.414	15.108	0.986
	5 Oct 2011	−13.010	17.251	21.606	13.878	0.973
	20 Oct 2011	0.184	7.565	7.567	4.807	0.966
	Average	−11.494	25.516	27.986	15.360	0.951
All Sites Average		2.836	37.870	39.472	25.591	0.936

GMDD
8, 2437–2495, 2015

Table 6. Daily simulation accuracy and average site simulation accuracy for *H* fluxes. Bias, scatter, RMSD and MAE are expressed in $W m^{-2}$. NASH index is unitless.

		Statistical Test				
Location	Date	Bias	Scatter	RMSD	MAE	NASH Index
Alice Springs	23 Mar 2011	−24.283	61.353	65.984	56.395	0.996
	15 Apr 2011	25.000	28.483	37.898	29.893	0.963
	23 Apr 2011	2.379	42.434	42.501	32.463	0.965
	10 May 2011	−24.020	64.040	68.397	53.226	0.975
	24 May 2011	9.203	27.768	29.253	24.611	0.921
	31 May 2011	−17.737	44.732	48.120	34.448	0.932
	18 Jun 2011	−16.026	37.981	41.224	28.271	0.983
	25 Jun 2011	−11.183	39.107	40.675	26.443	0.998
	18 Jul 2011	−7.949	28.681	29.762	22.792	0.999
	20 Aug 2011	−36.995	65.839	75.521	54.328	0.973
	Average	−10.161	49.352	50.387	36.287	0.970
Calperum	24 Feb 2011	58.725	62.785	85.968	69.624	0.981
	2 Mar 2011	4.584	46.737	46.961	35.209	0.963
	31 Mar 2011	8.700	42.428	43.311	30.601	0.899
	24 Apr 2011	67.405	72.419	98.934	74.959	0.991
	22 Jul 2011	−19.027	34.435	39.342	25.536	0.997
	28 Jul 2011	−1.208	32.853	32.875	25.318	0.998
	28 Aug 2011	−14.368	31.473	34.598	22.865	0.998
	1 Dec 2011	−20.735	38.835	44.023	36.183	0.986
	23 Dec 2011	−15.690	33.459	36.955	30.297	0.951
	29 Dec 2011	−12.294	38.799	40.700	32.767	0.932
	Average	5.609	54.526	54.814	38.336	0.970
Howard Springs	18 Apr 2011	56.780	50.308	75.861	58.880	0.995
	23 Apr 2011	24.083	34.731	42.264	29.461	0.996
	13 May 2011	69.810	67.245	96.930	70.172	0.995
	27 May 2011	12.165	32.135	34.360	24.116	0.973
	3 Jun 2011	12.112	42.248	43.950	30.034	0.963
	14 Jun 2011	19.126	46.531	50.309	34.010	0.932
	22 Jun 2011	−18.823	44.082	47.933	34.391	0.998
	22 Jul 2011	−9.049	26.807	28.293	19.520	0.937
	28 Jul 2011	−14.961	43.912	46.390	31.701	0.974
	27 Sep 2011	3.942	39.003	39.202	29.467	0.912
	Average	15.519	51.921	54.191	36.175	0.967
US_VAR	10 May 2011	37.638	40.409	55.222	41.198	0.889
	23 Jun 2011	−5.640	26.334	26.931	19.038	0.987
	19 Jul 2011	10.046	25.859	27.742	22.156	0.931
	30 Jul 2011	−7.480	31.142	32.028	23.875	0.847
	7 Aug 2011	11.298	24.187	26.695	21.235	0.869
	27 Aug 2011	29.359	37.648	47.742	37.527	0.899
	22 Sep 2011	34.803	28.526	45.000	38.054	0.899
	7 Oct 2011	29.169	25.739	38.901	30.290	0.997
	26 Nov 2011	28.168	32.328	42.878	30.923	0.984
	19 Dec 2011	13.813	18.958	23.457	19.175	0.994
	Average	13.817	33.477	38.065	28.347	0.930

GMDD
8, 2437–2495, 2015

Validating a 1-D SVAT model

G. P. Petropoulos et al.

Table 6. Continued.

Location	Date	Statistical Test Bias	Scatter	RMSD	MAE	NASH Index
US_MOZ	28 Jun 2011	−9.389	35.765	36.977	26.095	0.943
	1 Aug 2011	−34.096	58.247	67.493	44.072	0.926
	18 Aug 2011	18.999	35.006	39.830	29.074	0.911
	31 Aug 2011	−5.014	61.274	61.478	45.507	0.954
	1 Sep 2011	−14.392	60.862	62.541	47.645	0.938
	7 Sep 2011	−20.001	83.887	86.239	70.198	0.847
	12 Sep 2011	−1.372	45.672	45.692	36.452	0.970
	30 Sep 2011	−16.754	79.197	80.950	62.643	0.899
	29 Sep 2011	31.913	47.114	56.905	40.828	0.964
	11 Nov 2011	12.377	39.636	41.523	35.468	0.745
	Average	1.241	57.626	57.639	42.437	0.910
US_IB1	30 May 2011	43.822	42.735	61.210	55.528	0.912
	7 Jun 2011	−26.181	35.346	43.986	35.864	0.938
	28 Jun 2011	−21.756	24.512	32.774	26.233	0.981
	8 Jul 2011	27.469	13.964	30.815	27.469	0.987
	24 Aug 2011	66.892	39.502	77.685	67.519	0.949
	13 Sep 2011	40.239	33.828	52.569	43.639	0.945
	15 Sep 2011	44.111	35.651	56.717	44.872	0.974
	1 Oct 2011	70.614	49.184	86.054	70.614	0.960
	15 Oct 2011	20.106	36.150	41.365	31.272	0.958
	24 Oct 2011	36.481	24.821	44.124	36.853	0.987
	Average	30.180	46.557	55.483	43.986	0.959
US_TON	27 Feb 2011	−31.491	54.124	62.619	48.243	0.974
	17 Mar 2011	−32.302	53.987	62.913	41.689	0.949
	24 May 2011	20.698	66.336	69.490	50.301	0.891
	24 Jun 2011	−29.628	48.443	56.785	38.076	0.963
	30 Jul 2011	−26.672	65.907	71.099	49.319	0.964
	7 Aug 2011	−33.817	59.474	68.416	51.351	0.985
	28 Aug 2011	1.244	58.787	58.800	44.203	0.961
	15 Sep 2011	18.722	47.117	50.700	36.559	0.979
	1 Nov 2011	43.025	29.342	52.078	45.213	0.894
	16 Nov 2011	26.486	28.387	38.824	28.904	0.979
	Average	−4.374	59.770	59.930	43.386	0.954
US_WHS	8 Feb 2011	−18.241	59.823	62.542	47.839	0.896
	16 Feb 2011	−32.831	49.032	59.008	46.024	0.921
	25 Mar 2011	−27.278	38.850	47.470	38.025	0.973
	22 Jun 2011	−43.742	88.414	98.642	62.971	0.954
	13 Jul 2011	11.172	38.210	39.810	26.232	0.970
	2 Aug 2011	66.414	49.290	82.706	66.832	0.931
	28 Aug 2011	68.220	63.929	93.493	70.735	0.929
	3 Aug 2011	18.889	36.660	41.240	30.471	0.974
	5 Oct 2011	77.509	66.785	102.312	77.807	0.969
	20 Oct 2011	36.280	40.163	54.122	41.086	0.997
	Average	17.473	67.726	69.944	48.971	0.951
All Sites Average		8.663	52.619	55.057	40.140	0.951

GMDD
8, 2437–2495, 2015

Table 7. Daily simulation accuracy and average site simulation accuracy for T_{air} 1.3 m. Bias, scatter, RMSD and MAE are expressed in Celsius. NASH index is unitless.

		Statistical Test				
Location	Date	Bias	Scatter	RMSD	MAE	NASH Index
Alice Springs	23 Mar 2011	−1.193	1.806	2.164	1.873	0.822
	15 Apr 2011	0.558	2.604	2.663	1.989	0.842
	23 Apr 2011	3.698	1.867	4.142	3.717	0.839
	10 May 2011	−0.087	2.750	2.751	2.520	0.871
	24 May 2011	2.969	3.481	4.575	3.059	0.850
	31 May 2011	−1.660	2.201	2.757	2.365	0.927
	18 Jun 2011	−0.067	2.407	2.408	2.154	0.911
	25 Jun 2011	−2.966	2.675	3.994	3.341	0.915
	18 Jul 2011	−1.249	1.916	2.287	2.083	0.911
	20 Aug 2011	−0.334	2.103	2.129	1.926	0.917
	Average	−0.033	3.107	3.107	2.503	0.881
Calperum	24 Feb 2011	−3.281	2.677	4.235	3.686	0.874
	2 Mar 2011	0.821	2.256	2.401	1.675	0.914
	31 Mar 2011	1.010	3.313	3.463	2.654	0.886
	24 Apr 2011	−0.450	3.466	3.495	3.213	0.903
	22 Jul 2011	−2.557	1.582	3.007	2.607	0.904
	28 Jul 2011	−3.213	2.763	4.238	3.512	0.867
	28 Aug 2011	−7.921	3.432	8.633	7.977	0.791
	1 Dec 2011	−3.302	1.504	3.628	3.302	0.785
	23 Dec 2011	−5.545	2.908	6.262	5.642	0.833
	29 Dec 2011	−4.448	1.772	4.788	4.448	0.835
	Average	−2.889	3.759	4.741	3.872	0.859
Howard Springs	18 Apr 2011	1.803	0.882	2.007	1.855	0.743
	23 Apr 2011	−0.026	0.780	0.781	0.678	0.915
	13 May 2011	0.385	1.590	1.636	1.262	0.923
	27 May 2011	2.138	2.008	2.933	2.602	0.813
	3 Jun 2011	2.112	1.977	2.893	2.698	0.826
	14 Jun 2011	1.267	2.407	2.721	2.473	0.794
	22 Jun 2011	−0.976	1.898	2.134	2.014	0.871
	22 Jul 2011	0.166	2.140	2.146	1.816	0.888
	28 Jul 2011	−1.379	1.743	2.223	2.082	0.851
	27 Sep 2011	0.073	1.095	1.098	0.949	0.910
	Average	0.556	2.095	2.168	1.843	0.853
US_VAR	10 May 2011	−3.704	2.787	4.635	3.911	0.862
	23 Jun 2011	1.367	2.605	2.942	1.935	0.939
	19 Jul 2011	−0.694	2.342	2.443	2.161	0.927
	30 Jul 2011	2.525	3.338	4.185	3.212	0.915
	7 Aug 2011	0.551	2.848	2.901	2.265	0.933
	27 Aug 2011	−0.785	2.795	2.903	2.631	0.926
	22 Sep 2011	−3.777	2.988	4.816	4.144	0.884
	7 Oct 2011	0.082	2.949	2.950	2.731	0.846
	26 Nov 2011	1.927	1.489	2.436	1.994	0.863
	19 Dec 2011	1.424	1.280	1.915	1.562	0.890
	Average	−0.108	3.344	3.346	2.655	0.898

Table 7. Continued.

Location	Date	Statistical Test Bias	Scatter	RMSD	MAE	NASH Index
US_MOZ	28 Jun 2011	−0.702	0.749	1.026	0.972	0.821
	1 Aug 2011	1.671	1.043	1.970	1.682	0.909
	18 Aug 2011	−0.493	1.087	1.193	1.028	0.898
	31 Aug 2011	−0.973	1.207	1.550	1.234	0.903
	1 Sep 2011	3.873	2.581	4.654	3.873	0.631
	7 Sep 2011	1.144	1.668	2.023	1.450	0.890
	12 Sep 2011	1.731	0.914	1.958	1.731	0.883
	30 Sep 2011	0.695	2.026	2.142	1.787	0.830
	29 Sep 2011	−2.585	1.307	2.897	2.649	0.844
	11 Nov 2011	−1.697	2.119	2.715	2.451	0.924
	Average	0.226	2.373	2.383	1.844	0.853
US_IB1	30 May 2011	1.808	1.821	2.566	1.808	0.753
	7 Jun 2011	0.494	1.188	1.287	1.011	0.923
	28 Jun 2011	3.817	2.171	4.391	3.817	0.585
	8 Jul 2011	0.883	3.715	3.818	3.044	0.782
	24 Aug 2011	4.181	1.665	4.500	4.181	0.752
	13 Sep 2011	8.397	4.442	9.500	8.397	0.625
	15 Sep 2011	2.828	2.956	4.091	2.961	0.768
	1 Oct 2011	2.175	0.930	2.365	2.192	0.710
	15 Oct 2011	4.075	1.408	4.311	4.075	0.272
	24 Oct 2011	0.981	2.669	2.844	2.492	0.850
	Average	3.008	3.435	4.566	3.441	0.702
US_TON	27 Feb 2011	−1.681	0.938	1.925	1.713	0.833
	17 Mar 2011	−1.680	2.128	2.711	2.327	0.837
	24 May 2011	−0.692	1.344	1.512	1.183	0.922
	24 Jun 2011	1.506	1.355	2.025	1.789	0.906
	30 Jul 2011	1.470	2.030	2.507	1.856	0.923
	7 Aug 2011	3.114	2.781	4.175	3.114	0.875
	28 Aug 2011	2.084	2.423	3.196	2.115	0.919
	15 Sep 2011	4.263	3.146	5.298	4.289	0.788
	1 Nov 2011	1.272	2.138	2.488	2.266	0.873
	16 Nov 2011	0.385	0.955	1.030	0.824	0.919
	Average	1.004	2.768	2.944	2.148	0.880
US_WHS	8 Feb 2011	−1.320	1.920	2.330	2.050	0.901
	16 Feb 2011	0.786	1.893	2.050	1.794	0.869
	25 Mar 2011	−1.205	1.451	1.886	1.501	0.924
	22 Jun 2011	−0.564	2.594	2.655	2.072	0.880
	13 Jul 2011	2.255	2.244	3.181	2.979	0.745
	2 Aug 2011	0.553	1.373	1.480	1.173	0.907
	28 Aug 2011	0.648	1.350	1.498	1.197	0.940
	3 Aug 2011	2.764	4.309	5.119	4.266	0.739
	5 Oct 2011	0.557	1.226	1.347	1.106	0.934
	20 Oct 2011	−0.911	2.338	2.509	2.023	0.909
	Average	0.492	2.562	2.609	1.994	0.875
All Sites Average		0.282	2.930	3.233	2.540	0.850

Discussion Paper | Discussion Paper | Discussion Paper | Discussion Paper |

GMDD
8, 2437–2495, 2015

Validating a 1-D SVAT model

G. P. Petropoulos et al.

Title Page
Abstract Introduction
Conclusions References
Tables Figures
◀| |▶
◀ ▶
Back Close
Full Screen / Esc
Printer-friendly Version
Interactive Discussion

Table 8. Daily simulation accuracy and average site simulation accuracy for T_{air} 50 m. Bias, scatter, RMSD and MAE are expressed in Celsius. NASH index is unitless.

		Statistical Test				
Location	Date	Bias	Scatter	RMSD	MAE	NASH Index
Alice Springs	23 Mar 2011	−2.140	2.229	3.090	2.548	0.758
	15 Apr 2011	−0.048	3.101	3.101	2.706	0.785
	23 Apr 2011	3.492	2.908	4.544	3.492	0.849
	10 May 2011	−1.015	3.494	3.638	3.343	0.829
	24 May 2011	1.894	4.153	4.564	3.367	0.835
	31 May 2011	−2.588	3.052	4.001	3.323	0.898
	18 Jun 2011	−0.870	3.144	3.262	2.922	0.880
	25 Jun 2011	−3.605	3.414	4.965	3.957	0.899
	18 Jul 2011	−2.276	2.493	3.376	2.874	0.877
	20 Aug 2011	−1.275	3.006	3.265	2.950	0.872
	Average	−0.843	3.744	3.837	3.148	0.848
Calperum	24 Feb 2011	−4.351	3.875	5.826	4.912	0.833
	2 Mar 2011	0.148	3.030	3.034	2.576	0.868
	31 Mar 2011	0.783	4.356	4.426	3.770	0.837
	24 Apr 2011	−1.186	4.672	4.820	4.561	0.862
	22 Jul 2011	−2.085	2.807	3.497	2.726	0.900
	28 Jul 2011	−3.910	3.271	5.098	4.137	0.843
	28 Aug 2011	−8.457	4.515	9.587	8.763	0.771
	1 Dec 2011	−4.360	2.727	5.142	4.360	0.717
	23 Dec 2011	−6.684	3.535	7.561	6.780	0.800
	29 Dec 2011	−5.287	2.568	5.878	5.314	0.803
	Average	−3.539	4.572	5.782	4.790	0.823
Howard Springs	18 Apr 2011	0.847	1.203	1.471	1.067	0.852
	23 Apr 2011	−0.701	1.458	1.618	1.371	0.828
	13 May 2011	−0.515	1.573	1.656	1.474	0.910
	27 May 2011	2.135	1.186	2.442	2.151	0.845
	3 Jun 2011	1.915	1.067	2.192	1.916	0.876
	14 Jun 2011	0.817	1.070	1.347	1.201	0.900
	22 Jun 2011	−1.376	1.971	2.403	2.175	0.860
	22 Jul 2011	−0.386	2.240	2.274	1.932	0.881
	28 Jul 2011	−1.896	2.008	2.761	2.332	0.833
	27 Sep 2011	−0.299	1.651	1.678	1.442	0.863
	Average	0.054	2.036	2.037	1.706	0.865
US_VAR	10 May 2011	−4.690	3.778	6.023	5.167	0.818
	23 Jun 2011	0.642	3.978	4.030	3.185	0.899
	19 Jul 2011	−1.894	3.444	3.931	3.458	0.884
	30 Jul 2011	1.575	4.429	4.701	3.549	0.906
	7 Aug 2011	−0.429	4.004	4.027	3.422	0.898
	27 Aug 2011	−1.785	4.009	4.388	4.003	0.888
	22 Sep 2011	−4.330	4.062	5.937	4.891	0.863
	7 Oct 2011	−0.799	3.619	3.706	3.451	0.805
	26 Nov 2011	1.655	2.408	2.922	2.447	0.831
	19 Dec 2011	1.158	1.890	2.217	1.881	0.867
	Average	−0.890	4.243	4.336	3.545	0.866

Table 8. Continued.

Location	Date	Statistical Test Bias	Scatter	RMSD	MAE	NASH Index
US_MOZ	28 Jun 2011	−1.441	1.255	1.910	1.772	0.674
	1 Aug 2011	1.382	1.685	2.180	1.677	0.910
	18 Aug 2011	−1.438	1.695	2.223	1.828	0.819
	31 Aug 2011	−1.781	1.864	2.578	2.017	0.842
	1 Sep 2011	3.489	3.429	4.892	3.623	0.655
	7 Sep 2011	0.233	2.354	2.365	2.066	0.843
	12 Sep 2011	1.092	1.811	2.114	1.594	0.893
	30 Sep 2011	0.123	2.816	2.818	2.501	0.762
	29 Sep 2011	−3.443	1.577	3.787	3.443	0.798
	11 Nov 2011	−1.964	1.753	2.633	2.138	0.934
	Average	−0.458	2.809	2.846	2.219	0.813
US_IB1	30 May 2011	1.231	2.410	2.706	1.831	0.750
	7 Jun 2011	0.428	2.349	2.388	2.094	0.840
	28 Jun 2011	3.081	3.136	4.396	3.119	0.661
	8 Jul 2011	−0.192	4.092	4.096	3.608	0.741
	24 Aug 2011	4.358	3.287	5.459	4.358	0.741
	13 Sep 2011	8.203	5.501	9.877	8.203	0.491
	15 Sep 2011	1.856	3.835	4.260	3.317	0.740
	1 Oct 2011	1.761	1.500	2.313	1.761	0.767
	15 Oct 2011	4.103	2.343	4.725	4.103	0.267
	24 Oct 2011	0.325	3.171	3.188	2.842	0.829
	Average	2.515	4.113	4.821	3.524	0.683
US_TON	27 Feb 2011	−2.083	1.436	2.530	2.083	0.797
	17 Mar 2011	−1.977	2.839	3.459	2.930	0.795
	24 May 2011	−1.411	2.128	2.553	2.369	0.844
	24 Jun 2011	0.808	2.508	2.635	1.961	0.897
	30 Jul 2011	0.604	3.135	3.193	2.518	0.895
	7 Aug 2011	2.453	4.012	4.702	3.038	0.878
	28 Aug 2011	1.173	3.618	3.803	2.915	0.889
	15 Sep 2011	3.413	4.206	5.417	3.632	0.821
	1 Nov 2011	0.531	2.687	2.739	2.512	0.859
	16 Nov 2011	−0.126	1.572	1.577	1.489	0.853
	Average	0.338	3.417	3.434	2.545	0.853
US_WHS	8 Feb 2011	−1.428	2.637	2.999	2.651	0.872
	16 Feb 2011	1.147	2.017	2.320	1.792	0.870
	25 Mar 2011	−1.610	2.543	3.010	2.516	0.873
	22 Jun 2011	−1.001	3.040	3.200	2.806	0.838
	13 Jul 2011	1.249	2.594	2.879	2.208	0.811
	2 Aug 2011	−0.367	2.148	2.179	2.008	0.841
	28 Aug 2011	−0.318	2.103	2.127	1.938	0.903
	3 Aug 2011	1.842	4.702	5.050	4.157	0.746
	5 Oct 2011	−0.668	2.043	2.149	1.933	0.884
	20 Oct 2011	−1.431	3.130	3.442	3.018	0.864
	Average	−0.185	3.030	3.035	2.505	0.850
All Sites Average		−0.376	3.496	3.766	3.003	0.825

GMDD
8, 2437–2495, 2015

Validating a 1-D SVAT model

G. P. Petropoulos et al.

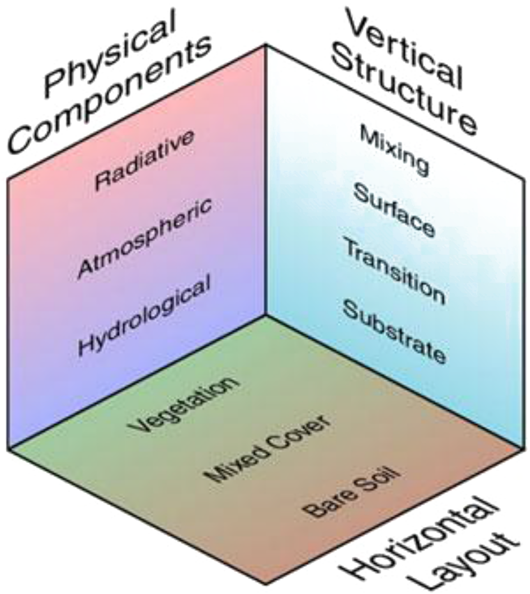

Figure 1. A simple representation of the SimSphere model architectural design.

GMDD
8, 2437–2495, 2015

Validating a 1-D SVAT model

G. P. Petropoulos et al.

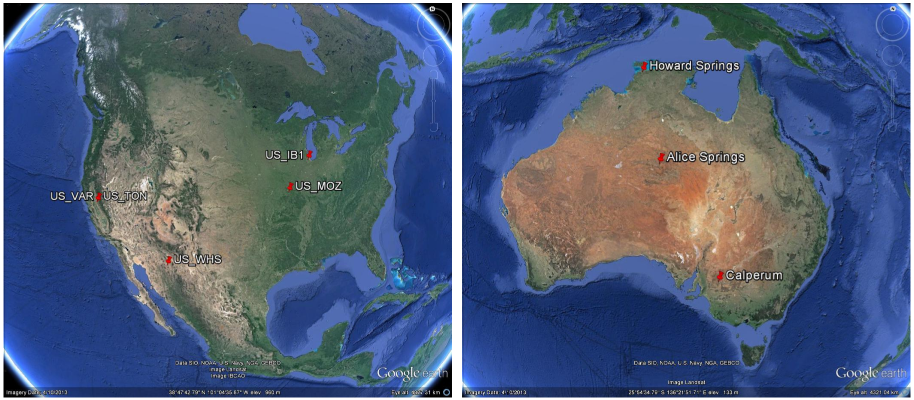

Figure 2. Maps of site location taken from Google Earth.

GMDD
8, 2437–2495, 2015

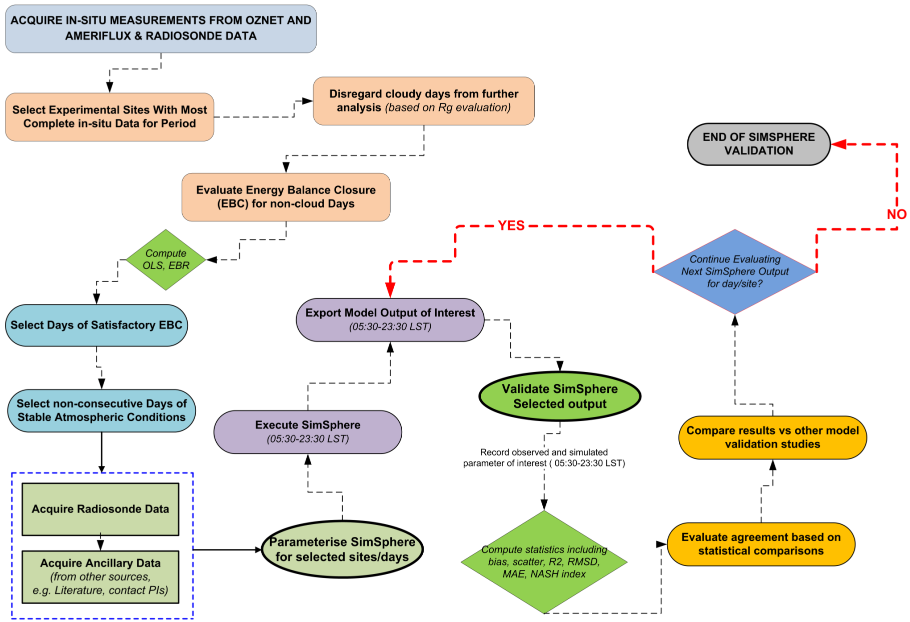

Figure 3. Flowchart of the overall methodology followed.

GMDD

8, 2437–2495, 2015

Validating a 1-D SVAT model

G. P. Petropoulos et al.

Title Page
Abstract | Introduction
Conclusions | References
Tables | Figures
◀| |▶
◀ ▶
Back | Close
Full Screen / Esc
Printer-friendly Version
Interactive Discussion

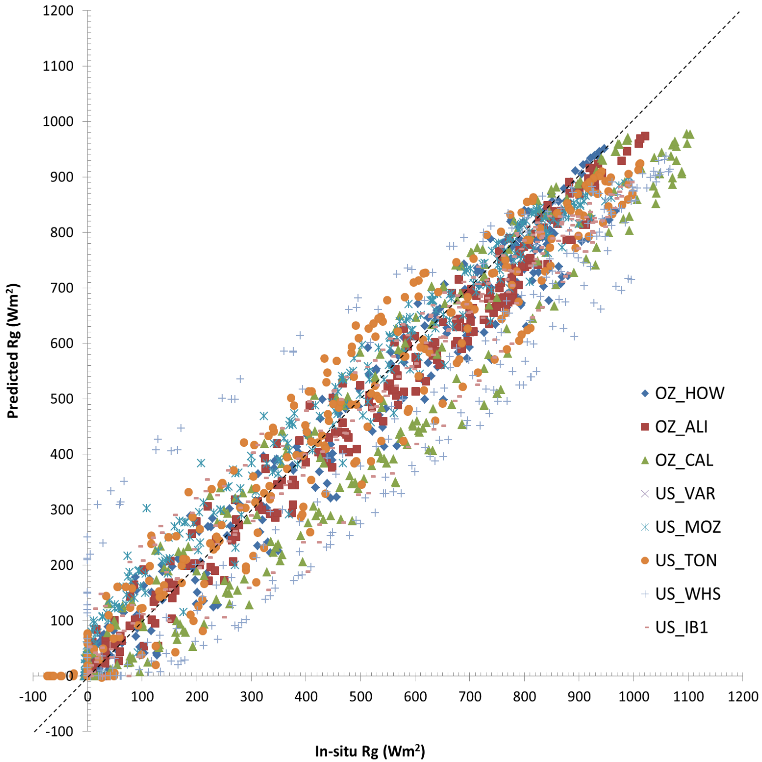

Figure 4. Scatterplot comparison of SimSphere predicted and in situ R_g flux.

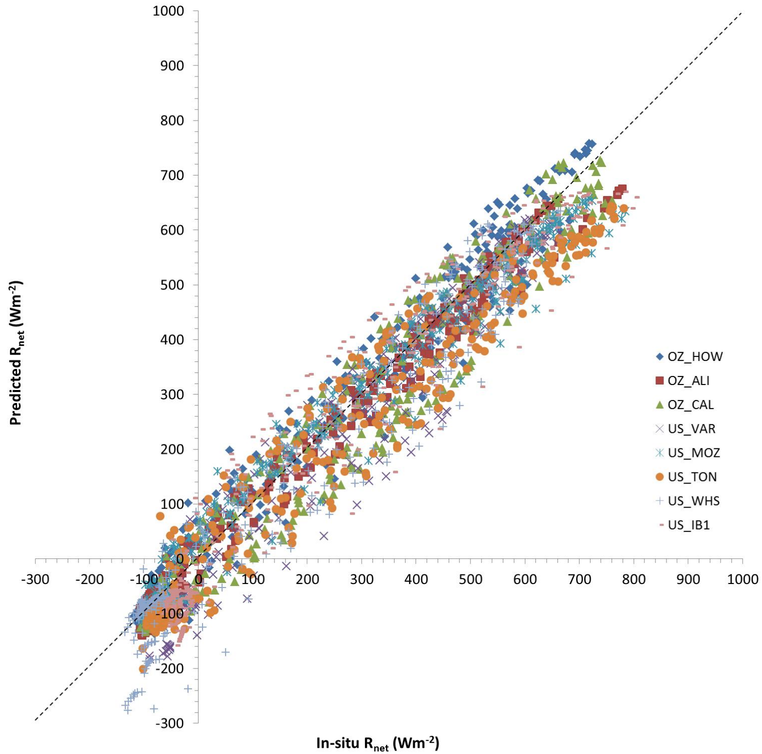

Figure 5. Scatterplot comparison of SimSphere predicted and in situ R_{net} flux.

GMDD
8, 2437–2495, 2015

Validating a 1-D SVAT model

G. P. Petropoulos et al.

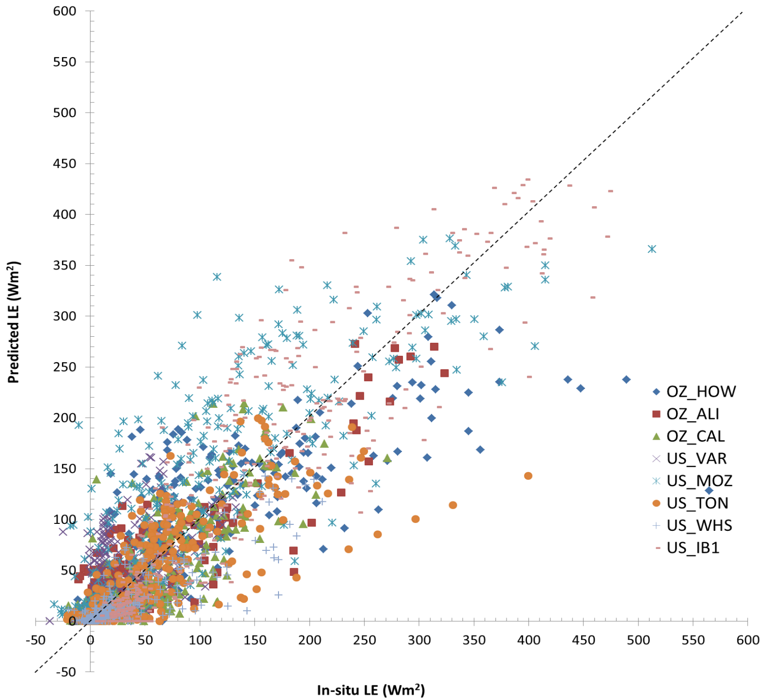

Figure 6. Scatterplot comparison of SimSphere predicted and in situ LE flux.

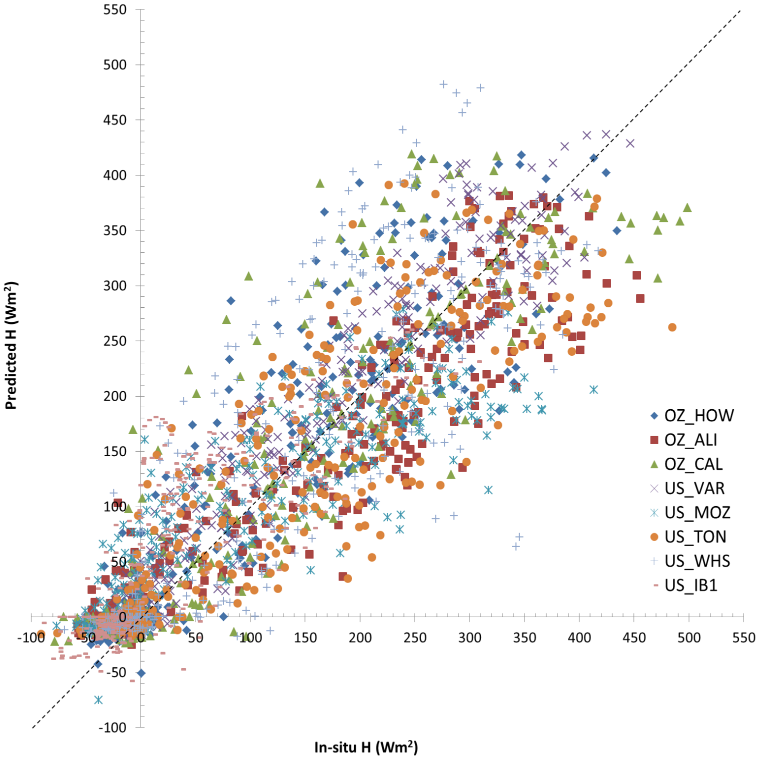

Figure 7. Scatterplot comparison of SimSphere predicted and in situ *H* Flux.

GMDD
8, 2437–2495, 2015

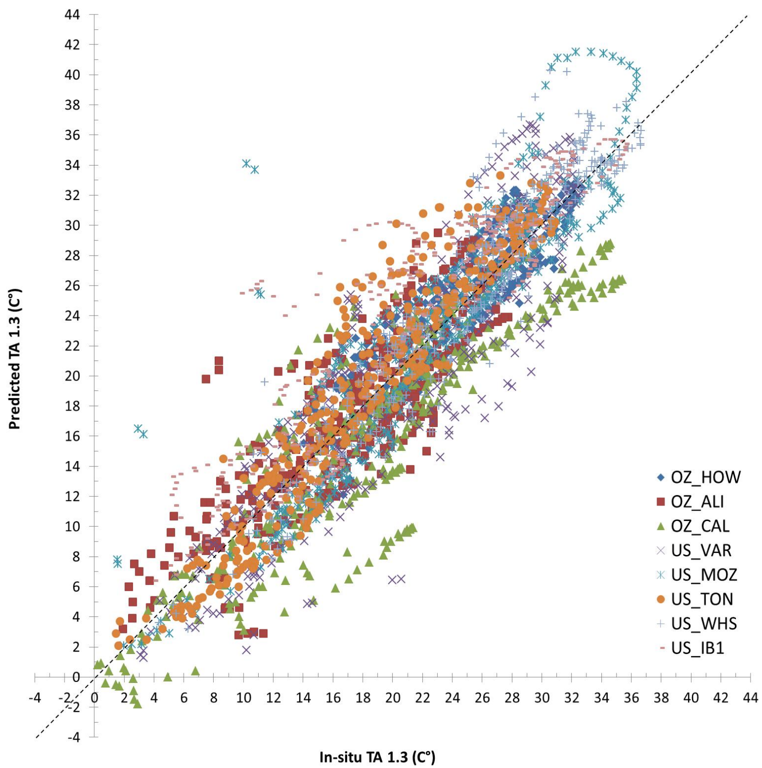

Figure 8. Scatterplot comparison of SimSphere predicted and in situ $T_{air1.3\,m}$.

GMDD
8, 2437–2495, 2015

Validating a 1-D SVAT model

G. P. Petropoulos et al.

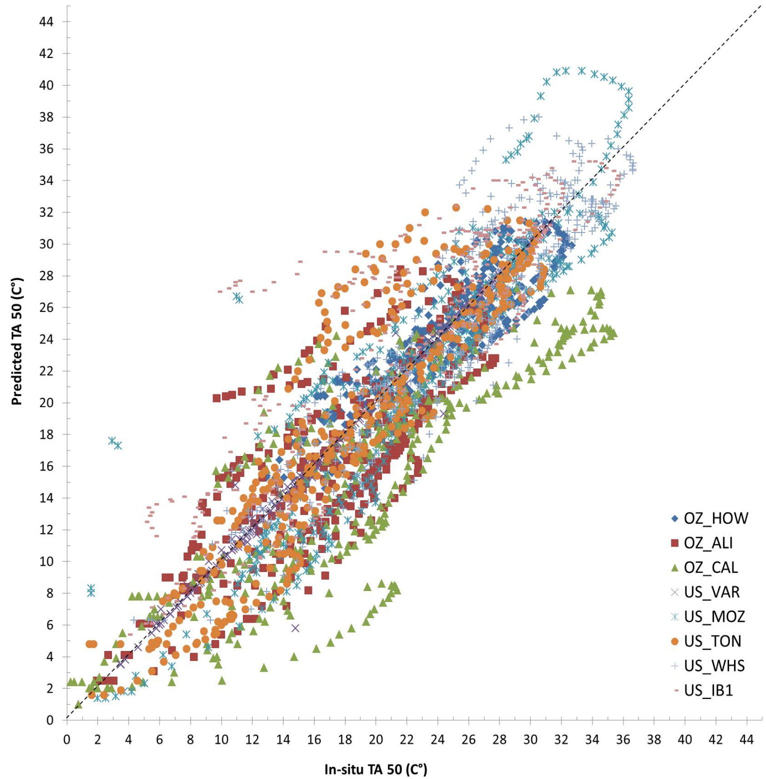

Figure 9. Scatterplot comparison of SimSphere predicted and in situ $T_{\mathrm{air50\,m}}$.